

NATIONAL RADIO ASTRONOMY OBSERVATORY
CHARLOTTESVILLE, VIRGINIA

ELECTRONICS DIVISION INTERNAL REPORT No. 145

ROOM TEMPERATURE AND CRYOGENIC MIXERS
FOR 80 - 120 GHz

A. R. KERR

JULY 16, 1974

NUMBER OF COPIES: 150

ROOM TEMPERATURE AND CRYOGENIC MIXERS

FOR 80 - 120 GHz

A. R. Kerr

ABSTRACT

Design and construction details are given for new room temperature and cryogenic mixers operating from 80 to 120 GHz. The room temperature mixer achieves a single sideband conversion loss of 5.5 dB with a single sideband noise temperature of 500 °K (excluding the IF contribution), measured at 115 GHz. The corresponding quantities for the cryogenic mixer are 5.8 dB and 300 °K. Both mixers use gallium arsenide Schottky barrier diodes, which are mounted in two new types of waveguide mount.

ROOM TEMPERATURE AND CRYOGENIC MIXERS

FOR 80 - 120 GHz

A. R. Kerr

TABLE OF CONTENTS

<u>ABSTRACT</u>	(i)
<u>TABLE OF CONTENTS</u>	(ii)
1. <u>INTRODUCTION</u>	1
2. <u>THEORETICAL CONSIDERATIONS</u>	2
2.1 The Simplified Model	2
2.2 The Mixing Process	6
2.3 Mixer Design	9
2.4 A Design Example	9
3. <u>ACCURATE ANALYSIS OF THE MIXER</u>	12
3.1 An Improved Model of the Diode Mount	12
3.2 The Diode Waveform	13
3.4 A Proposed Approach to Mixer Analysis	15
4. <u>MEASUREMENTS ON MIXERS AND THEIR INTERPRETATION</u>	17
4.1 Instrumentation, Measurement Procedure, and Terminology	17
4.2 Measurements on Broadband Mixers	21
5. <u>MIXER DESIGN DETAILS AND CONSTRUCTION</u>	26
5.1 A Room Temperature 3 mm Mixer	26
5.1.1 Waveguide Transformer	26
5.1.2 Diode Mount	29
5.1.3 Backshort	36
5.1.4 Performance	36

5.2	A Cryogenic 3 mm Mixer	37
5.2.1	Waveguide Transformer	38
5.2.2	Main Block	41
5.2.3	Backshort and Drive	43
5.2.4	IF Transformer	44
5.2.5	Performance	46
6.	<u>DIODE FABRICATION AND CONTACTING</u>	47
6.1	Diodes	47
6.2	Contact Whiskers	49
6.2.1	Diode Contacting -- Room Temperature Mixers	49
6.2.2	Diode Contacting -- Cryogenic Mixers	51
6.3	Fabrication of the Quartz Diode Mounts	52
6.3.1	Photolithographic Choke Fabrication	53
6.3.2	Cutting the 0.006" Quartz	53
6.3.3	Bonding to the Quartz	54
6.3.4	Mounting the Chip	54
6.3.5	Mounting and Bending the Whisker	55
6.3.6	Assembling the Three Quartz Pieces	55
7.	<u>REFERENCES</u>	58
	<u>APPENDIX 1: MOUNT THE MATCHING CURVES</u>	A 1
	<u>APPENDIX 2: BANDWIDTH CURVES</u>	A 4
	<u>APPENDIX 3: CONVERSION LOSS DEGRADATION CURVES</u>	A 7
	<u>APPENDIX 4: PHOTOLITHOGRAPHY ON CHROME-GOLD QUARTZ</u>	A10

ROOM TEMPERATURE AND CRYOGENIC MIXERS

FOR 80 - 120 GHz

A. R. Kerr

1. INTRODUCTION

This report covers the work done on millimeter-wave mixers at NRAO between August 1971 and February 1974. The aim of the project was to develop better mixers for receivers used in radio astronomy, and to investigate the potential of cryogenically cooled mixers. Our initial investigation of cryogenic mixers was published^[1] in February 1973 and is not reiterated in detail here.

The best mixers available for the 80-120 GHz range in 1971 had single-sideband noise temperatures of 2000-3000 °K. These used "Sharpless Wafer" diode mounts of the kind developed at Bell Labs^[2] in the 1950's, and Schottky barrier diodes on epitaxial gallium arsenide. Our early investigations led us to abandon the Sharpless wafer in favor of an improved structure for the following reasons:

(i) The epoxy-supported RF choke section of the IF lead is several quarter-wavelengths long at RF, which imposes a restriction on its useful bandwidth. Strong RF leakage out of the IF connector was observed at certain frequencies with several commercial wafers.

(ii) The capacitance of the RF choke becomes difficult to tune out over a broad IF bandwidth, especially at high IF frequencies (~5 GHz) which were used in the cryogenic receiver work.

In chapter 2 a theoretical investigation of the impedance matching of mixers, both at RF and at IF, is made. This suggests using very much reduced waveguide height; 1/4 of the standard height rather than the conventional 2/3 or 1/2. A simplified model of the mixer is assumed, and predicted impedance

levels are realized within a factor of two. The limitations of this model, and a more accurate one are discussed in Chapter 3, and techniques described for solving the nonlinear problem of determining the actual diode waveforms.

Chapter 4 describes the techniques used to make measurements on mixers, and interprets some interesting results.

Chapters 5 and 6 give the construction details of the mixers and diodes, respectively, which yielded single sideband noise temperatures* of 500 and 300 °K at room temperature and 18 °K, respectively.

2. THEORETICAL CONSIDERATIONS

2.1 The Simplified Model

For want of a better model it has become conventional to represent a waveguide mounted diode as shown in Fig. 2.1(a). This model assumes the diode mounting structure to be electrically short in the direction of propagation in the waveguide, and also that connections to the diode at DC and IF are completely bypassed for the RF energy in the waveguide.

It is usual to terminate the waveguide on one side of the diode in an adjustable short-circuit; in Fig. 2.1(b) the susceptance B represents this "back-short" as seen from the plane of the diode. On the other side of the diode the input to the mixer is represented by the waveguide characteristic impedance as given by Schelkunoff: [3]

$$Z_g = 2 \sqrt{\frac{\mu}{\epsilon}} \cdot \frac{b}{a} \cdot \frac{1}{\sqrt{1 - \left(\frac{fc}{f}\right)^2}} \quad (2.1)$$

* These temperatures exclude the IF noise contribution.

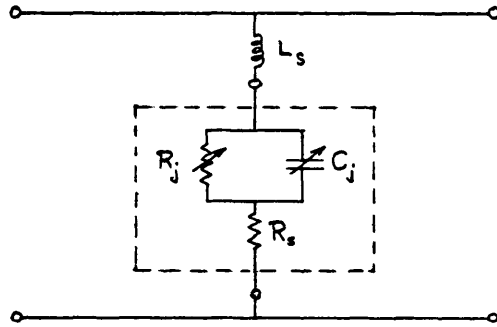


FIG 2.1(a)

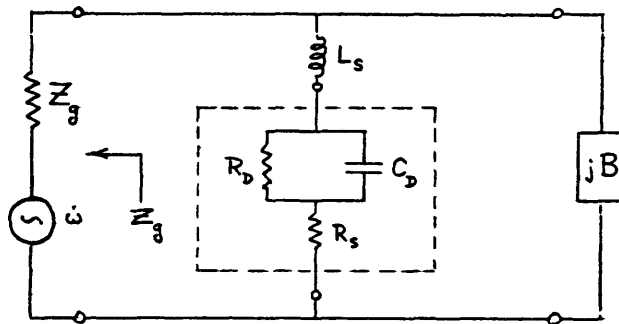


FIG 2.1(b)

where b and a are respectively the waveguide height and width, and the other symbols have their conventional meanings. Schelkunoff also produced a formula for the inductance of a wire across the centre of a waveguide, which he communicated privately to Sharpless: [2]

$$L_s = 2 \times 10^{-7} b \log_e \left(\frac{2a}{\pi r} \right) \text{ Henry} \quad - (2.2)$$

where r is the radius of the wire, and the waveguide height b is in metres.

It should be noted that this formula applies only to a thin straight wire connected directly between the upper and lower walls of a waveguide, and it should not be expected to apply with great accuracy to the situation where a diode is connected in series with the wire; this is discussed in more detail in Chapter 3.

Elements R_D , C_D , and R_S represent the diode as it appears at the signal frequency when local oscillator drive is applied to it. It is tacitly assumed that R_D and C_D will be the same at the image frequency as at the signal frequency -- a fairly reasonable assumption when the intermediate frequency is very low compared with the local oscillator frequency.

When the mixer is operating optimally the values of R_D and B should be adjusted to match as much as possible of the signal power from Z_g into R_D . If all the elements in Fig. 2.1(b) are fixed, except for R_D and B , there will in general be two values of B for which the impedance seen by R_D is real. That is, there are two values of R_D for which the mount can be matched by tuning the backshort.*

As a first step in designing a mixer it is useful to know how the pairs of values of R_D and B , required for matching, vary with C_D , L_S , and R_S . A computer program, MATCH2, was written to calculate the values of B and R_D for which R_D is matched -- other element values in Fig. 2.1(b) are held constant. A typical set of results is shown in Fig. 2.2, and sets of results covering a wide range of parameter values are given in Appendix 1. In these graphs impedances are normalized to the waveguide impedance, Z_g . The mean junction

* Note that matching of R_D in this way only guarantees maximum power transfer from Z_g to R_D if $R_S = 0$. In this section it is assumed that although $R_S \neq 0$, nearly maximum power transfer will occur when R_D is matched to its embedding circuit.

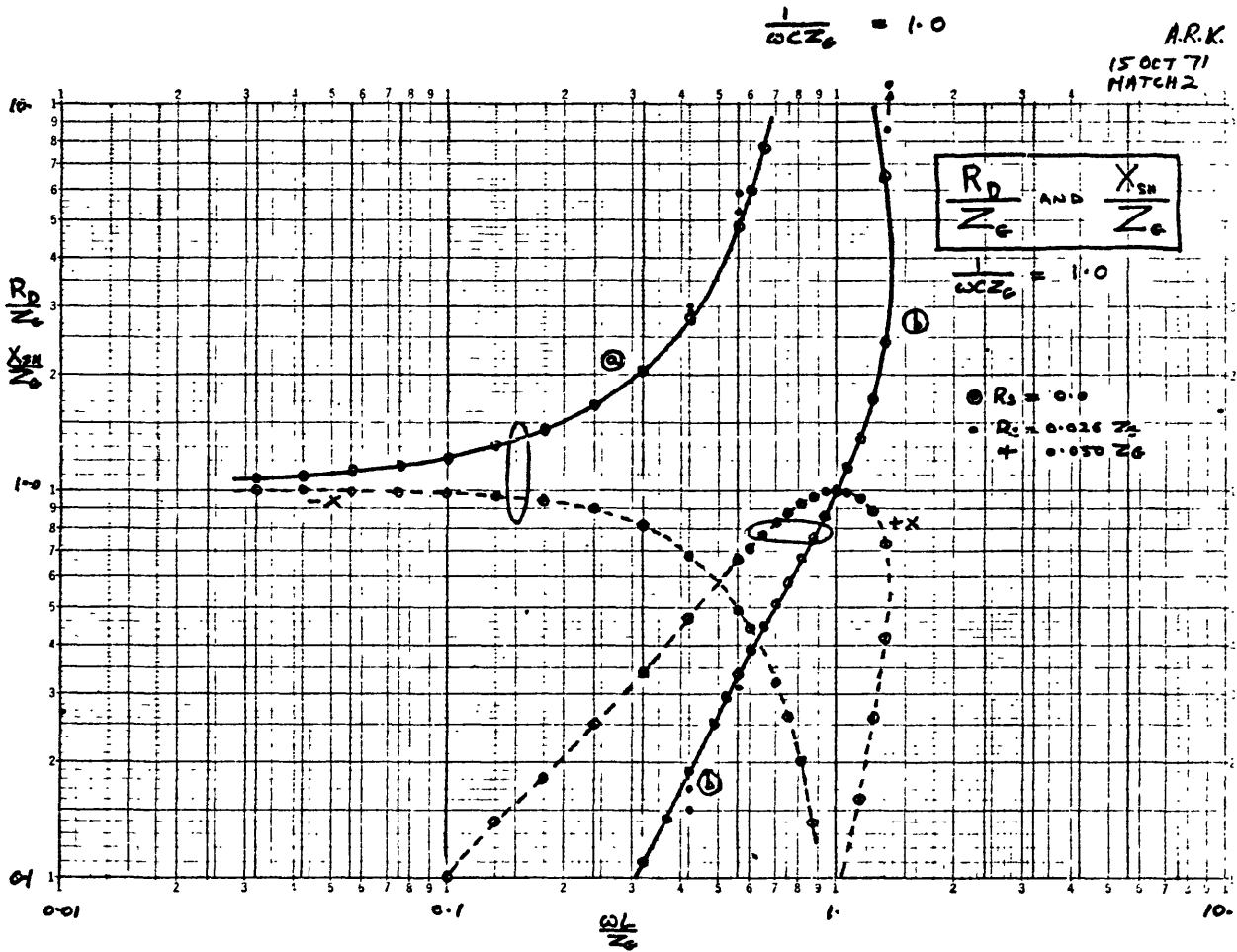


FIG 2.2

capacitance C_D is set for each graph, and curves are drawn for $R_s = 0$; typical points are plotted for other values of R_s to indicate the deviation of the curves from those for $R_s = 0$. The abscissa is the normalized lead reactance $\frac{\omega L_s}{Z_g}$, and the ordinates are $\frac{R_D}{Z_g}$ and $\frac{X_{sh}}{Z_g}$ (where $X_{sh} \triangleq \frac{-1}{B}$). Thus the graphs show the values of R_D and B , for which matching to R_D is obtained, as a function of ω and L_s .

An interesting result of these curves is that in the range of values of

$\frac{\omega L_s}{Z_g}$ and $\frac{1}{\omega C_D Z_g}$ expected for our 3mm mixers, the two values of R_D for which a match is obtainable may differ by more than an order of magnitude. In the next section it will be shown that the IF impedance, Z_{if} , is largely a function of the RF impedance seen by the diode. Thus, for a given mixer it may be possible to adjust the backshort and LO drive to give two matched operating conditions for which the values of Z_{if} differ widely.

The bandwidth associated with each set of points on the matching curves has been calculated, and the results are plotted in the graphs of Appendix 2. These curves give the 1 dB fractional bandwidth of the power coupling from the RF source impedance, Z_g , into the diode resistance R_D , assuming a fixed backshort setting. In practice one requires this bandwidth to be greater than

$\left(\frac{2f_{IF}}{f_{LO}} \right)$ in order that both upper and lower sidebands fall within the band.

In Appendix 3 the Conversion Loss Degradation Factor, D , is plotted with the same parameters as the matching and bandwidth graphs. The factor D accounts for the part of the conversion loss of the mixer due to power dissipated in the diode's series resistance R_s . The best broadband mixer, with an ideal LO waveform, can never have a conversion loss L less than $2D$, i.e., in decibel quantities

$$L(\text{dB}) \geq 3\text{dB} + D(\text{dB}).$$

2.2 The Mixing Process

In much of the work on mixer theory that has been published since Torrey and Whitmer's^[4] original analysis, it has been assumed that the exponential diode is driven by a large sinusoidal local oscillator voltage. In fact the voltage waveform across an exponential diode in a mixer circuit is far from sinusoidal,* as has been demonstrated by Barber,^[5] and by Fleri and Cohen.^[6]

* This is obvious if one considers the finite source impedance of the local oscillator in series with the nonlinear diode.

The actual voltage and current waveforms that exist in a real mixer circuit depend on the nonlinearity of the diode's resistance and capacitance, and on the embedding impedance seen by the diode at the harmonics of the LO frequency.

To determine conversion loss and IF impedance of the mixer it is required that the impedance seen by the diode at all the frequencies ($nf_{LO} \pm f_{IF}$) be known in addition to the diode current and voltage waveforms. For a practical millimeter-wave mixer it is difficult to calculate the embedding impedances at frequencies much above the LO frequency because the waveguide and RF choke structures become multi-moded.*

We have then two difficult problems to solve before an exact analysis of a given mixer can be made: (i) determining the diode waveforms, and (ii) determining the embedding impedance at many harmonically related frequencies.

There is, however, a way to circumvent these problems in designing a mixer if certain design parameters are able to be determined by experience. To this end it will now be assumed that the mixer consists of a diode mounted centrally in a reduced height waveguide, an effective RF choke in the DC/IF connection to the diode, and a backshort in the waveguide behind the diode. The effect of the waveguide height, contact inductance, and diode capacitance and resistance can be studied using the approximate RF equivalent circuit described in the previous section, and the required value of R_D , the mean diode resistance when operating as a mixer, can be established for each set of the variables. It is also possible, thanks to the work of A. Saleh,^[7] to deduce upper and lower bounds on the IF impedance required for each set of variables.

Saleh^[7] has considered resistive mixers in four categories, depending on

* One approach to this problem, which is being studied at the time of writing, is to measure these embedding impedances on a low frequency model of the diode mount.

the termination of the image and related out-of-band frequencies. He has studied the effects of various LO waveforms, including sinusoidal, square, and rectangular pulse, on the mixer conversion loss and input and output impedances. In all the cases he has covered there is never more than a factor of $\frac{\pi^2}{4}$ (≈ 2.5) difference between the optimum source (RF) and load (IF) impedances, and in most cases the factor is between 1 and 2 when the diode is reasonably hard driven by the LO. This gives us the useful inequality relating Z_{IF} to Z_{RF}

$$2.5 Z_{RF} \geq Z_{IF} \geq \frac{Z_{RF}}{2.5} \quad (2.3)$$

A simple example of the implications of this inequality is given by considering a low frequency waveguide mixer in which the lead inductance is relatively small. Then the diode impedance is matched directly to the waveguide characteristic impedance. For full height waveguide this is ~ 400 Ohms, so the IF impedance required to match the mixer will be between 160 and 1000 Ohms. These figures are born out in practice by the range of IF impedances found in typical lower frequency waveguide mixers.*

For a mixer operating with a broad IF band it is desirable that the IF impedance should be as close as possible to the input impedance of the IF preamplifier -- 50 Ohms in all cases to be considered here. If the IF impedance of the mixer is too far from preamplifier impedance, the required matching circuit will introduce unnecessary loss and IF bandwidth restriction. It is clear then from equation 2.3 that we should aim at a mixer for which the diode sees an RF impedance of $\sim 50\Omega$. The optimum IF impedance should then lie between 20 and 125 Ohms, for which a broadband circuit for matching to 50 Ohms is easily

* See for example the Alpha Industries catalog, which gives typical IF impedances for their Schottky mixer diodes.

realized.

2.3 Mixer Design

The previous two sections have established approximately the RF coupling between the diode and the input waveguide, and the relationship between the IF and RF impedances of the diode in the presence of LO drive. It was shown that by designing the mount to present an RF impedance of about 50 Ohms to the diode, the IF impedance might be expected to be sufficiently close to 50 Ohms for easy matching to be achievable over a useful bandwidth.

Assuming a value of the mean diode capacitance C_D [Fig. 2.1(b)], it is possible to use the graphs in Appendix 1, together with equations 2.1 and 2.2 relating Z_g and L_s to waveguide height b , to determine the optimum waveguide height. In most cases the result will indicate that a very much reduced-height waveguide is required, which may be mechanically difficult. However, as will be shown in the example below, a 1/4 height waveguide can give good mixer performance while being mechanically feasible. This is a considerably greater height reduction than conventionally used for millimeter wave mixers; usually 1/2 to 2/3 height guide has been used.

2.4 A Design Example

Consider the mixer design shown in Fig. 2.3. The waveguide is reduced height WR-10 (75-110 GHz), the height being 1/4 of the standard height, which is as low as possible with a semiconductor chip thickness of ~0.006" and a whisker length of ~0.006". The RF matching curves in Appendices 1, 2, 3 will be used to predict the performance of this mixer using two different Ga As Schottky barrier diodes whose characteristics are tabulated below. It will be assumed that the mean value of the diode capacitance [C_D in Fig. 2.1(b)] is equal to its zero bias value.

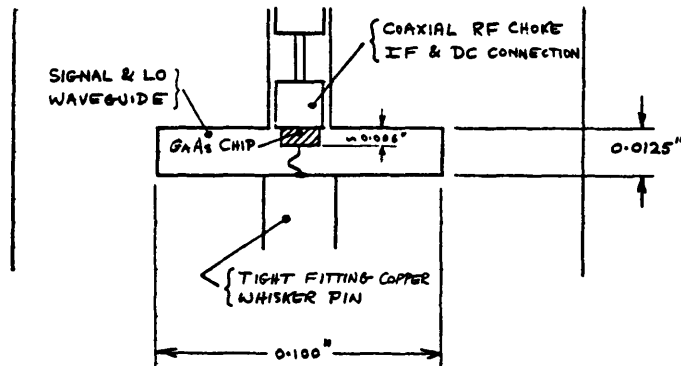


FIG 2-3

DIODE AND MOUNT PARAMETERS AT 100 GHz

Diode	2.5 micron Ga As	3.5 micron Ga As
C_o measured at 1 MHz	0.007 pF	0.020 pF
R_s	8 Ohm	3.5 Ohm
L_s from Eq. 2.2	0.17 nH	
Z_g from Eq. 2.1	117 Ohm	
$X_L = \omega L$	107 Ohm	
$\frac{X_L}{Z_g} = \frac{\omega L}{Z_g}$	0.92	
$X_c = \frac{1}{\omega C_o}$	227 Ohm	80 Ohm
$\frac{X_c}{Z_g} = \frac{1}{\omega C_o Z_g}$	1.94	0.69
$\frac{R_s}{Z_g}$	0.068	0.030

From the graphs in Appendices 1, 2 and 3 we find the following results:

PREDICTED MIXER CHARACTERISTICS

Diode	2.5 micron	3.5 micron
Impedance seen by diode when mount is tuned	176 <u>OR</u> 190 Ohm	120 <u>OR</u> ~1000 Ohm
Conversion Loss Degradation D dB	0.2 dB	0.5 <u>OR</u> ~10 dB
1 dB Bandwidth of RF Matching	70%	30% <u>OR</u> ~0%

Measurements on a number of mixers using both the 2.5 and 3.5 micron diodes have given the following typical results:

MEASURED MIXER CHARACTERISTICS

Diode	2.5 micron	3.5 micron
IF Impedance	80 Ohm	100 Ohm
Conversion Loss L dB single sideband (theoretical min. is 3 dB)	5.5 dB	6.7 dB
T_{MXR_SSB} (single sideband receiver noise temp. less IF contribution)	500 °K	1360 °K

The results in the tables show that the IF impedances do lie within the range given by equation 2.3. The conversion losses of the two mixers differ by more than the 0.3 dB difference in degradation factors; this is probably due to the different terminations seen by the out-of-band sidebands ($n f_{LO} \pm f_{IF}$), $n \neq 0$ or 1, and also to the different local oscillator current and voltage waveforms for the two diodes. No measurements were made of the instantaneous

bandwidth.

3. ACCURATE ANALYSIS OF THE MIXER

3.1 An Improved Model of the Diode Mount

It has been shown by Eisenhart and Khan^[8] that the simplified model of the waveguide-mounted diode, shown in figure 2.1(b), is far from accurate in many cases. Schelkunoff's equations for Z_g and L_s , as used by Sharpless, are not accurately applicable to the problem. By computing the coupling between the diode terminals and each mode in the waveguide it is possible to obtain an accurate value for the driving point impedance seen by the diode. Both TE and TM modes must be considered, and evanescent modes (i.e., below cutoff) must not be ignored since they still have energy storage and will contribute reactively. By considering 20 each TE and TM modes, Eisenhart and Khan have computed driving point impedances in close agreement with their measured values up to frequencies as high as seven times the waveguide cutoff frequency.

For analysing a mixer mount it is theoretically possible to use this method to determine the impedance of the diode's embedding network at all the frequencies of interest: i.e., nf_{LO} , and $(nf_{LO} \pm f_{IF})$. The impedances at the harmonics of the LO frequency will, together with the diode's large signal characteristics, determine the voltage and current waveforms at the diode. An accurate computer procedure for achieving this is described in the next section. Having determined the diode waveforms and the embedding impedance at frequencies $(nf_{LO} \pm f_{IF})$, $n \neq 0$, computation of the mixer's conversion loss and IF impedance is straightforward using the conversion impedance matrix approach.^[4]

3.2 The Diode Waveform

The "simple" problem of analysing the circuit shown in Fig. 3.1 turns out to be surprisingly difficult because of the very strong nonlinearity

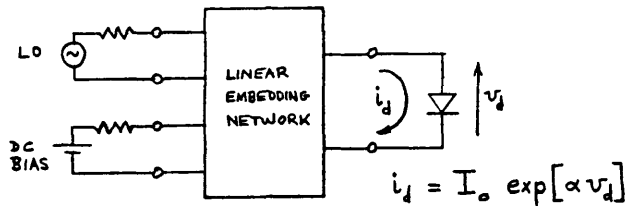


FIG 3.1

of the diode. Several approaches were tried but in most cases it was found that the solution either failed to converge, or was so slowly convergent as to be impracticable. This was found to be the case with Newton's method^[9] in which perturbations are made in each harmonic of the diode current, and the network equations examined to see whether the perturbation has brought the system closer to a solution. The harmonics are then adjusted as indicated by their perturbations and the new current tested. For cases where only 2 or 3 harmonics were considered convergence was sometimes achieved (see Ref. 10), but with 10 harmonics the results were seldom convergent.

A new approach was tried based on the fact that once the steady state is achieved for the circuit of Fig. 3.1, a length, ℓ , of transmission line of arbitrary characteristic impedance, Z_0 , can hypothetically be inserted between the diode and the embedding network, as shown in Fig. 3.2. Provided ℓ

is an integral number of half wavelengths at the LO frequency the presence of the transmission line will not change the i_d and v_d waveforms. This is not to say that the mixer performance will be the same under these conditions, but only that the LO waveform at the diode will be unchanged.

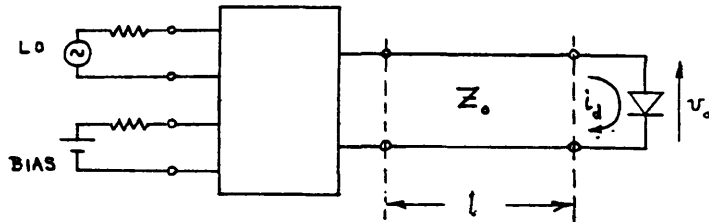


FIG 3.2

The turn-on transient when LO power is first applied to the circuit will consist of a series of reflections between the diode and the embedding network. Clearly if l is made a very large number of half-wavelengths at the LO frequency, the equilibrium between the diode and transmission line will be closely approached following the arrival of each new reflection at the diode. During this period of equilibrium a reflection from the diode will propagate back down the transmission line, and be reflected yet again from the embedding network, to form the next wavefront incident on the diode. Since in the physical situation the solution converges to the final desired solution as more and more reflections occur, so in the computer simulation convergence also ultimately occurs. On each iteration an additional reflection at the diode is considered. This simply entails solving the problem depicted in Fig. 3.3, which is relatively straightforward in the time-domain. The reflected frequency components from the diode are then calculated by taking the Fourier transform of $v_d(t)$, and

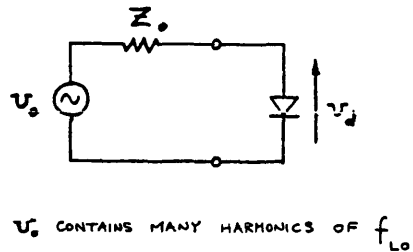


FIG 3.3

the reflection at the embedding network computed in the frequency-domain.

This technique was tested for the simplified equivalent circuit of Fig. 2.1(b) and found to converge in about 50 cycles of iteration when 10 harmonics of the LO frequency were considered. The choice of Z_o affects the rate of convergence to some extent, but it was found that for the cases considered a choice of 50 to 100 Ohms was near optimum.

3.3 A Proposed Approach to Mixer Analysis

The model of the waveguide mounted diode discussed in Section 3.1 must be extended in the practical situation to include the non-ideal RF choke structure in the DC and IF circuit, and the non-ideal "backshort" in the waveguide behind the diode.

In millimeter wave mixers it is difficult to make the RF choke structure so small that it will be invisible to a wave travelling along the guide. Although the choke may be effective when excited from the diode, its finite electrical length along the waveguide will appear as a discontinuity,^[11] and should be represented as shown in Fig. 3.4(b). Fig. 3.4(a) shows the simplified equivalent circuit which applies to an electrically thin choke structure.

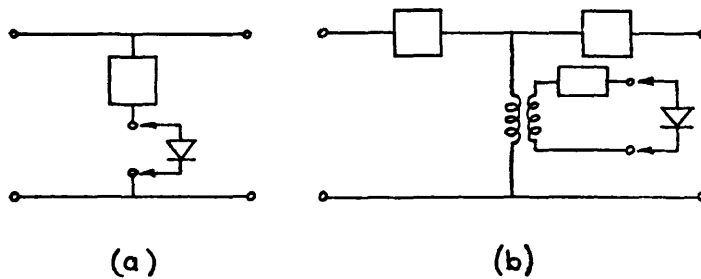


FIG 3-4

In addition to this electrical length effect, the RF choke will normally be designed to be effective in the vicinity of the LO frequency, but at harmonics of the LO the choke will no longer present a short circuit at the waveguide wall, nor will it behave as a simple TEM-mode structure. Higher mode propagation will be possible in the choke, and in fact there will be a strong excitation of the coaxial TE_{11} mode because of the electrical asymmetry of the mount caused by the presence of the backshort behind the diode.

The backshort is usually adjustable, and is designed to reflect the TE_{10} mode. By using a backshort which completely blocks the waveguide, all modes will see a high reflection coefficient; however, because of the desirability of using spring-finger contacts against the broad surfaces of the waveguide, the electrical plane of the short-circuit will probably vary considerably from one mode to the next.

The implication of the preceding three paragraphs is that although the equivalent circuit model of Section 3.2, and the choke equivalent circuit of Fig. 3.4(b) are useful for computing the mount characteristics at the signal and LO frequencies, at harmonics of the LO frequency they become inapplicable.

The most direct solution to this problem appears to be to use low frequency scale models of proposed mounts to study the impedance of the mount as seen by the diode at all frequencies of interest.* The measured impedance data and the particular diode characteristics could then be analysed by computer to determine the diode voltage and current waveforms, and the small-signal parameters of the mixer -- i.e., conversion loss, IF impedance, etc. This procedure is presently being further developed by the author at the Goddard Institute for Space Studies.

4. MEASUREMENTS ON MIXERS AND THEIR INTERPRETATION

4.1 Instrumentation, Measurement Procedure, and Terminology

The noise and conversion loss measurements given in this report were performed using the IF noise radiometer/reflectometer system described by Weinreb and Kerr,^[1] shown in Fig. 4.1. The system operates at the IF frequency

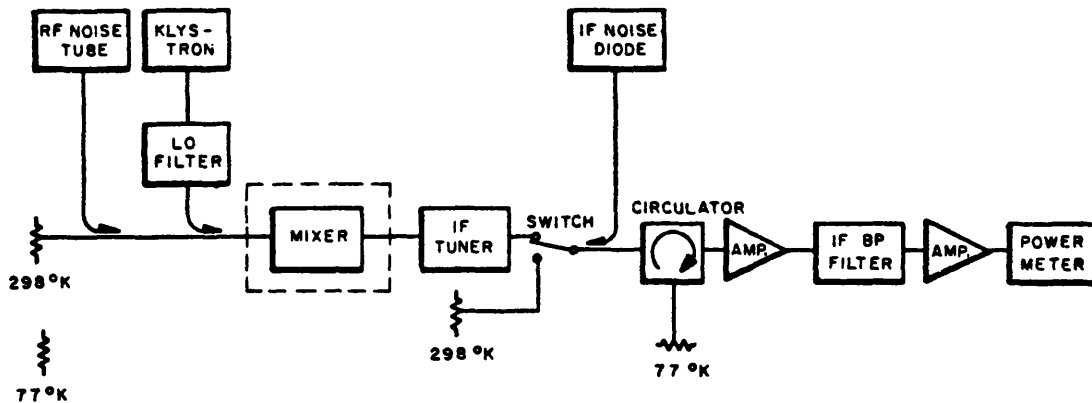


FIG 4.1

* To use this scale model as an actual mixer is not feasible because of the impracticability of frequency scaling the properties of the Schottky barrier diodes.

of 1.4 or 4.75 GHz, and gives a direct reading, in degrees Kelvin, of the temperature seen at the IF port of the mixer under test. A solid state noise source and a high directivity directional coupler allow a high level (~6000 °K) noise signal to be directed at the IF-port of the mixer, and the fraction of this power reflected back into the radiometer gives the magnitude of the reflection coefficient. A calibrated millimeter wave noise source, or cold load at the RF input of the mixer enables the conversion loss to be measured directly, and the measurements of IF-port temperature and match enable the mixer's noise temperature to be calculated. The detailed measurement procedure is as follows:

- 1) The RF noise tube and directional coupler are calibrated against room temperature and liquid nitrogen loads. This is accomplished using a mixer and the IF measuring system together as a millimeter wave power level indicator.
- 2) The IF measuring system is calibrated using liquid nitrogen and room temperature loads.
- 3) The mixer's IF noise temperature is measured with the RF noise tube both on and off.
- 4) The IF match is measured by injecting the 6000 °K from the noise diode towards the IF-port of the mixer, and noting the power reflected.
- 5) The conversion loss is calculated from the known RF and IF temperature increments when the RF noise-tube is switched on. Correction is made for the loss due to IF mismatch.
- 6) The IF temperature is corrected for noise from the IF measuring system that is reflected back into the IF measuring system by the IF mismatch.
- 7) The mixer's contribution to the system noise is calculated.

It is appropriate here to define some terms and symbols as they are used

in this report. All quantities are single-sideband unless otherwise explicitly noted. The single-sideband system noise temperature of a receiver can be expressed as:

$$\begin{array}{rccccccc}
 T_S & = & T_A & + & T_i \left(\frac{L}{L_i} \right) & + & T_{MXR} & + & L T_{IF} \\
 \text{total system} & & \text{antenna noise} & & \text{antenna noise} & & \text{mixer noise} & & \text{IF noise} \\
 \text{noise} & & \text{in signal band} & & \text{due to image band} & & \underbrace{\hspace{10em}} & & \\
 & & & & & & \text{receiver noise} & & \\
 & & & & & & T_R & &
 \end{array} \quad (4.1)$$

where T_A and T_i are respectively the antenna temperatures at the signal and image frequencies, T_{IF} is the noise temperature of the IF amplifier, and T_{MXR} is the single-sideband noise temperature of the mixer. L and L_i are the signal and image conversion losses of the mixer: for a broadband mixer $L = L_i$.

The frequently used noise temperature ratio, t , of the mixer is related to T_{MXR} by:

$$T_{MXR} = T_O \left(tL - 1 - \frac{L}{L_i} \right) \quad (4.2)$$

where $T_O = 290$ °K. The writer believes that T_{MXR} is more appropriate than t for characterizing a mixer, as it gives the mixer's contribution to the system noise, independent of L .

One further quantity which is helpful in characterizing a mixer, is the temperature, T_L , of a passive, lossy 3-port network, equivalent to the mixer in all respects except that no frequency conversion occurs.* Ports 1, 2, and 3 correspond to the

* Weinreb and Kerr^[1] have assumed T_L to be equal to $T_{D_{AV}}$, the average diode temperature. However, since the measured quantity T_L includes noise contributions from sources other than just the diode, i.e., from mount losses and higher sidebands, and is strongly reduced by the presence of RF mismatch as explained in Section 4.2, it seems more accurate to think of T_L as an average temperature associated with the net loss of the mixer, and quite distinct from $T_{D_{AV}}$.

signal, image, and IF-ports, respectively, of the mixer. The relation between T_L and T_{MXR} is derived with the aid of Fig. 4.2 showing the equivalent lossy 3-port.

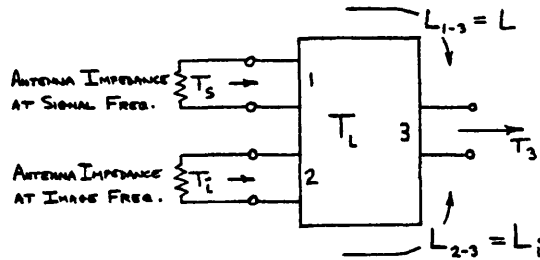


FIG 4.2

$$T_3 = \frac{T_s}{L} + \frac{T_i}{L_i} + \frac{T_{MXR}}{L} \quad (4.3)$$

Now let $T_s = T_i = T_L$. Then from the second law of thermodynamics T_3 must be equal to T_L : so in equation 4.3

$$T_L = \frac{T_L}{L} + \frac{T_L}{L_i} + \frac{T_{MXR}}{L}$$

$$\therefore T_{MXR} = T_L \left(L - 1 - \frac{L}{L_i} \right) \quad (4.4)$$

For the broadband mixer with $L = L_i$ this reduces to

$$T_{MXR} = T_L (L - 2) \quad (4.4a)$$

It should be noted at this point that the assumed equivalence between the mixer and a lossy 3-port network has tacitly implied that the mixer is a recip-

rocal device. This is not necessarily the case, since for reciprocity to apply in a mixer, the conductance waveform of the diode, $g(t)$, must be able to be expressed as an even function of time by a suitable choice of time origin. Computed and analog measurements on models of Schottky diode mixers have shown that this is not generally the case. In practice, however, it seems that the assumption of reciprocity does not lead to significant inconsistencies.

4.2 Measurements on Broadband Mixers

In Figures 4.3 and 4.4 measurements at 85 and 115 GHz of L , T_L , and T_{MXR} , as functions of the back-short position, are shown for a typical good mixer. The values of these parameters were measured, as described above, with the IF-port unmatched, and corrected to give values which would be obtained under matched conditions.* The optimum operating point for a mixer is near the minimum of the T_{MXR} curve: if a low noise IF amplifier (e.g., paramp) is used, this operating point will give minimum system noise temperatures.

An interesting observation from these graphs is that at the optimum operating point, T_L measured at 85 GHz is almost twice its value at 115 GHz. The low frequency performance is still superior to the high frequency performance because of the lower conversion loss and T_{MXR} . This observation has been made for many different diodes: mixers which have lower L and T_{MXR} usually have higher values of T_L .

An explanation of this phenomenon is given below in terms of the matching

* These corrected values have been checked in several cases against measurements made with an IF matching transformer in the circuit, and good agreement have been obtained.

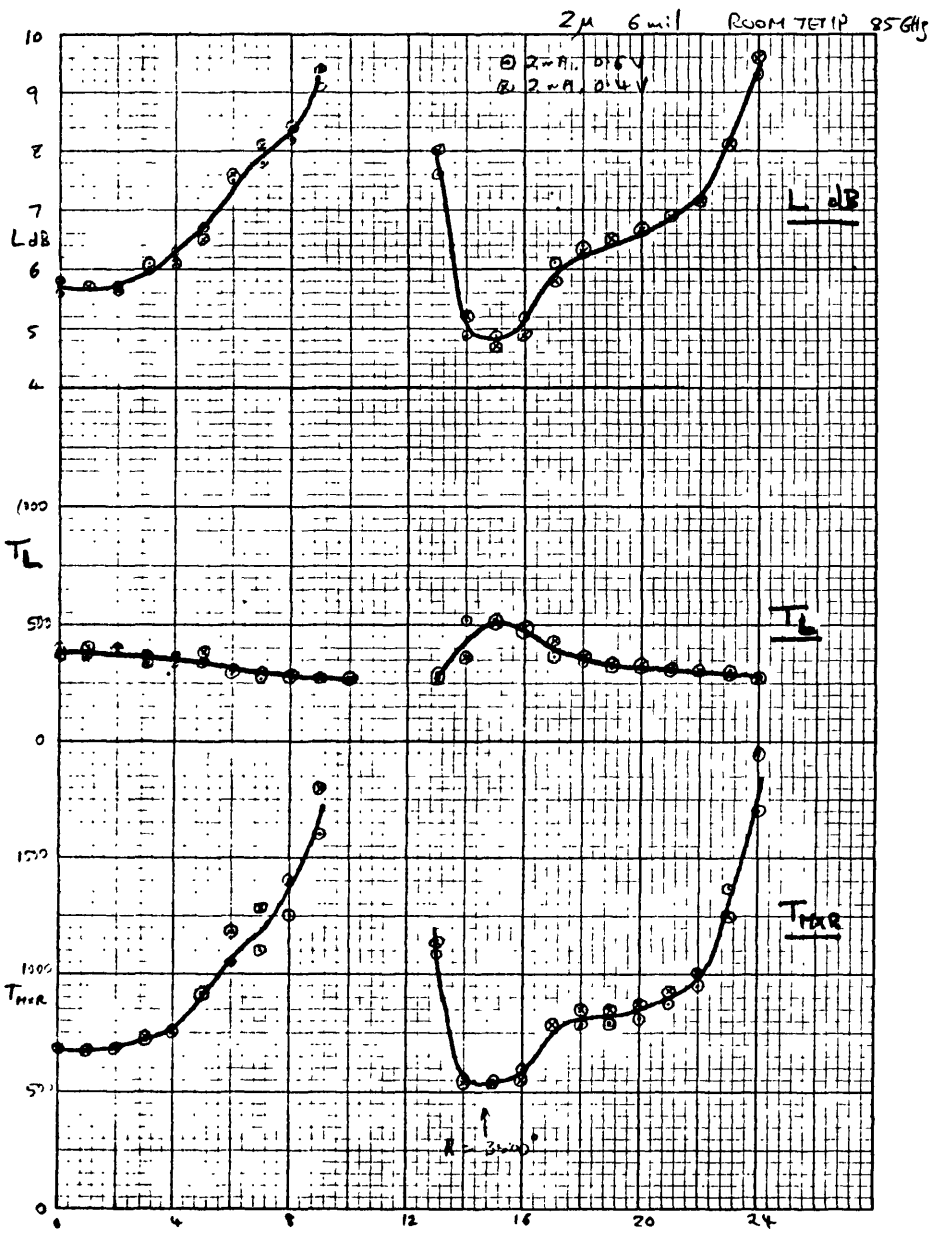


FIG 4.3

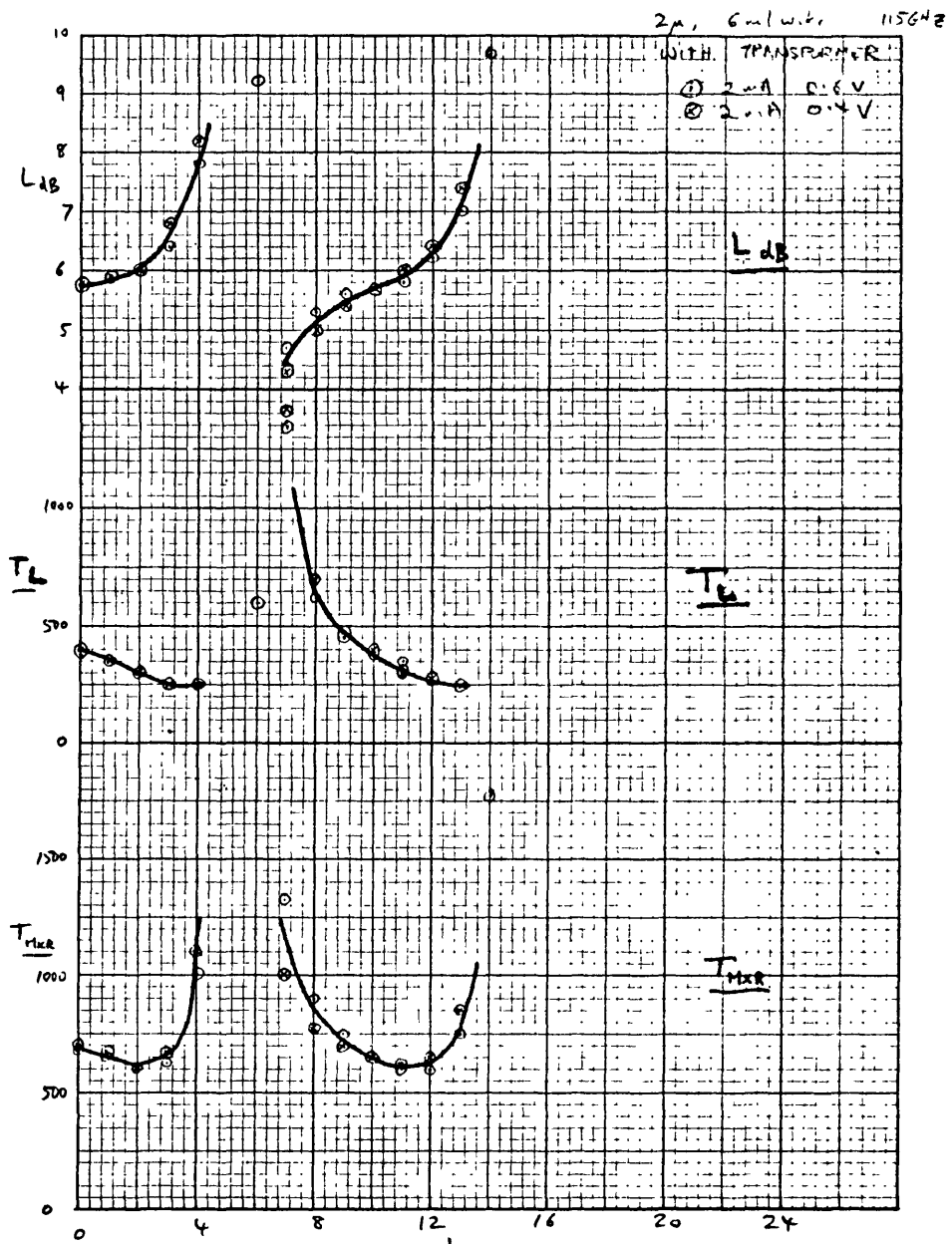


FIG 4.4

of the RF input of the mixer. The explanation of the very high values of T_L , ~500 °K for a room temperature mixer, and ~200 °K for a cryogenically cooled mixer, is not apparent. The possibilities of noise generation due to reverse breakdown of the diode, or due to parametric action of the diode's junction capacitance, are currently being investigated.

To explain the observed dependence of T_L on mixer performance it is necessary to consider the RF matching of the mixer. Consider a matched broad-band mixer as shown in Fig. 4.5. The signal and image input temperatures,

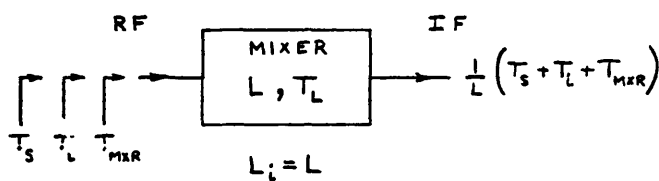


FIG 4.5

T_s and T_i , give an output at the IF-port $\frac{1}{L} (T_s + T_i)$. There is an additional output term due to the mixer's self-noise: $\frac{1}{L} \cdot T_{MXR}$, where T_{MXR} and T_L are related by equation 4.4(a).

Now let a reflective mismatch be introduced in the input circuit of the mixer as shown in Fig. 4.6. Then for the system taken as a whole, the effective values of conversion loss, T_{MXR} , and T_L are:

$$L_{\text{eff}} = \frac{L}{1 - |\rho|^2} \tag{4.5}$$

$$T_{\text{MXR}}^{\text{eff}} = \frac{T_{\text{MXR}}}{1 - |\rho|^2} \tag{4.6}$$

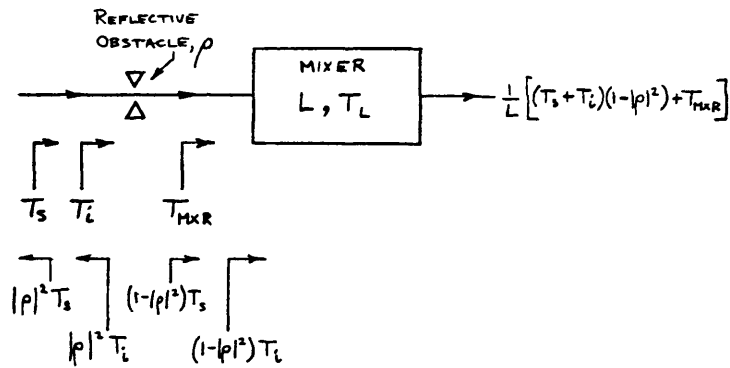


FIG 4.6

and

$$T_{L_{eff}} = \frac{T_{MXR_{eff}}}{L_{eff} - 2}$$

$$= T_L \cdot \frac{L - 2}{L - 2(1 - |\rho|^2)} \tag{4.7}$$

The implication of this is that introducing a reflection in the input of a matched mixer will not only increase the effective values of L and T_{MXR} , but will also reduce the effective value of T_L . This may explain the observed tendency for poor mixers to have lower values of T_L , as described above.

The introduction of the reflecting obstacle into the RF circuit (Fig. 4.6) will have caused the IF match to change, and some recovery of L and T_{MXR} will be possible by re-matching the IF-port. However, the improvement will be small relative to the original degradation.

To demonstrate the effect of an RF circuit mismatch on L and T_L , curves are shown in Fig 4.7 which relate L_{eff} , L , $T_{L_{eff}}$ and T_L for different values

of $|\rho|^2$. As an example: a mixer with an RF input VSWR of 3:1 ($|\rho|^2 = 0.25$) has an excess conversion loss of 1.25 dB and will indicate a value of $T_{D_{eff}}$ which is 0.7 to 0.85 times the maximum value. Improved IF matching will recoup a small fraction of the increase in conversion loss.

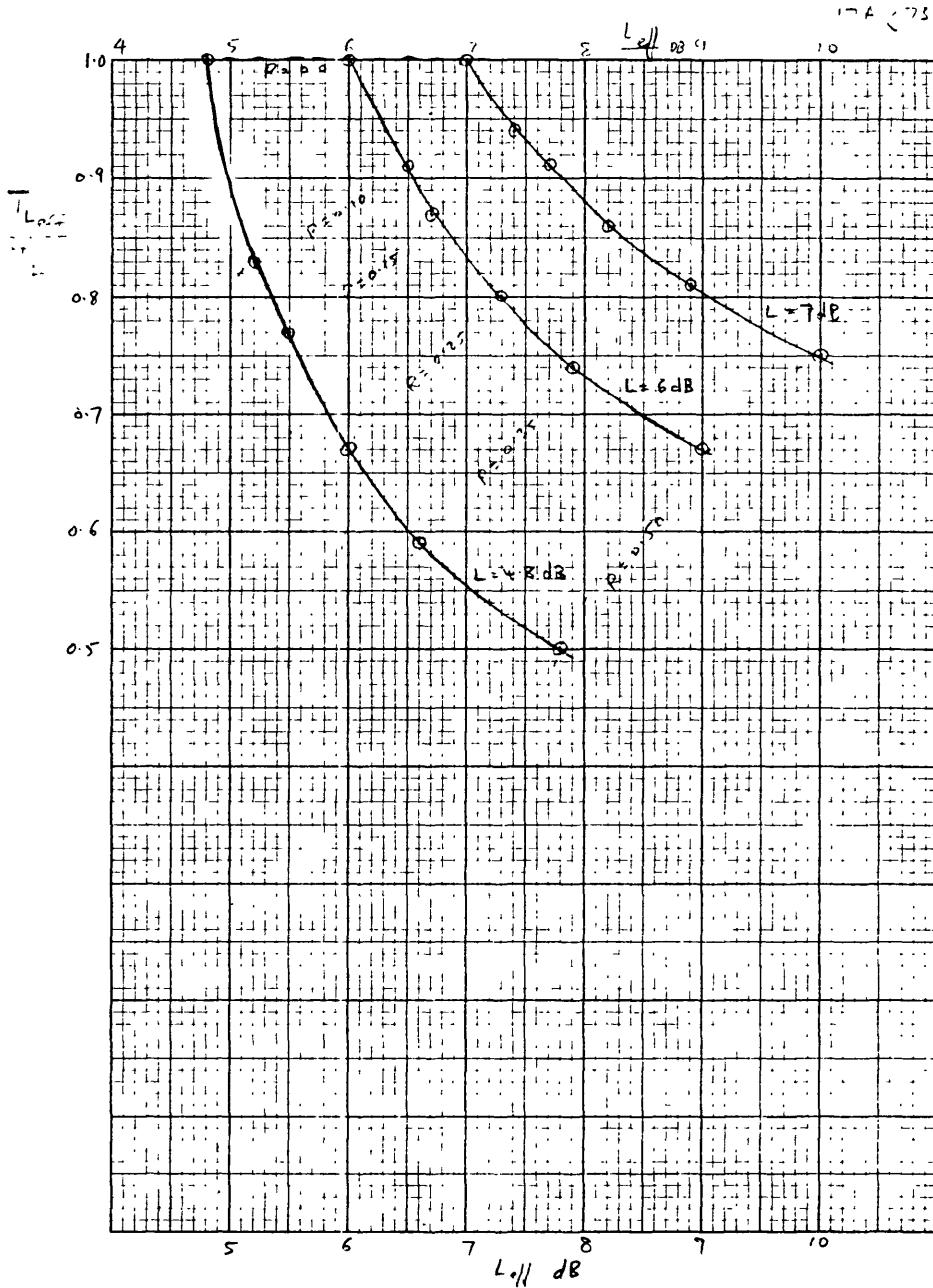


FIG 4.7

Direct measurement of the small-signal input match of a millimeter wave mixer is difficult because of the presence of the high level LO power in the input circuit, and has not been attempted in this work. The conventional assumption that a good LO match implies a good RF match is not correct. [12]

5. MIXER DESIGN DETAILS AND CONSTRUCTION

5.1 A Room Temperature 3 mm Mixer

The design is based on that described in Section 2.4. The mixer consists of three main parts: a stepped waveguide transformer, the diode mount, and the backshort with its drive mechanism. Figure 5.1 shows the assembly in cross section, not to scale.

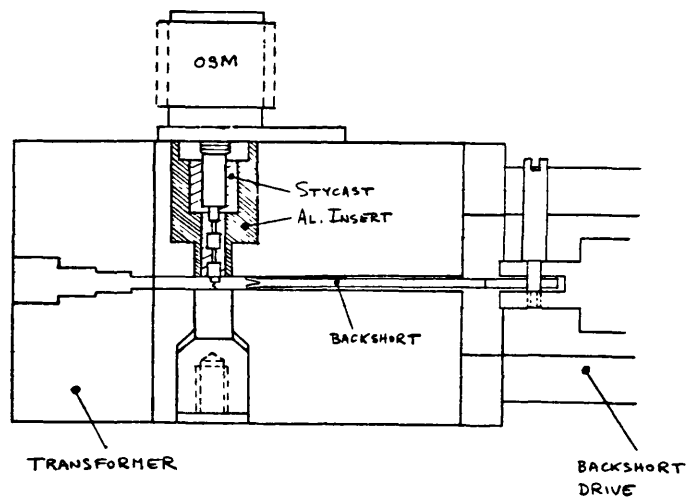


FIG 5.1

5.1.1 Waveguide Transformer

The waveguide transformer is designed to have a low reflection over the band 80-120 GHz. The choice of a stepped structure over a taper was

20-120 GHz TRANSFORMER

ELECTROFORMING MANDREL

6061 ALUMINUM

MAKE 4

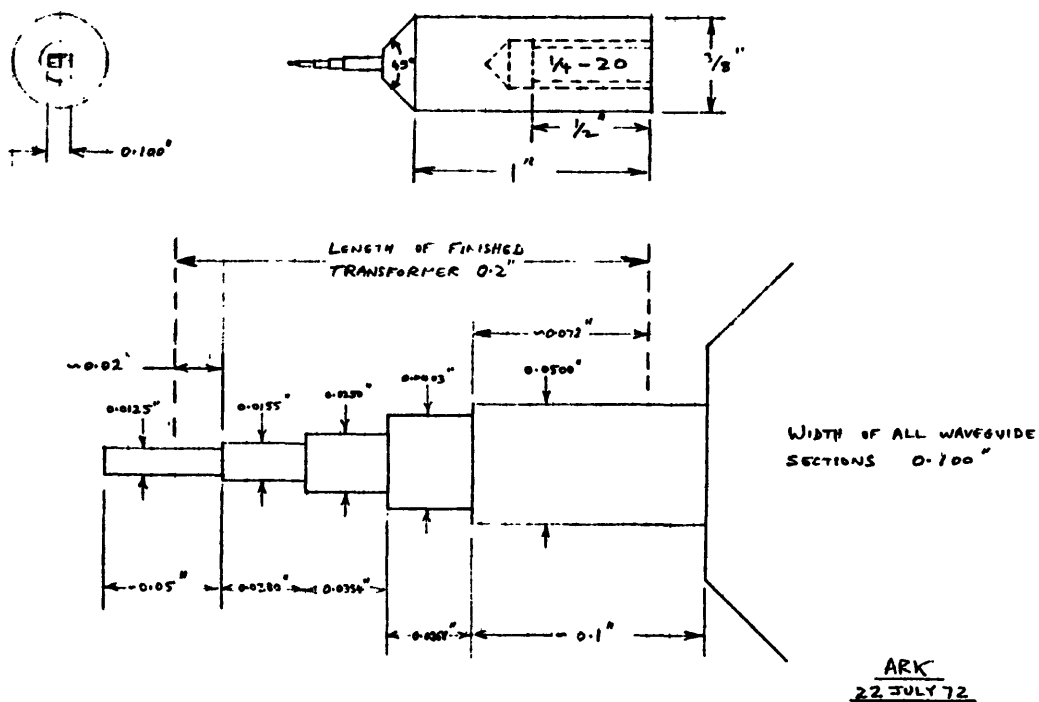


FIG 5.2

based on: (i) the shorter length of the stepped structure compared with a linear taper of the same bandwidth, and the resulting lower loss; and (ii) the greater ease of fabrication of the stepped transformer over any tapered section. The design is based on the procedure given by Matthaei, Young, and Jones^[13] p. 276 and predicts a VSWR of ≤ 1.06 across the band.

An aluminum mandrel was milled to the dimensions given in Fig. 5.2, and this was gold plated and then copper electroformed until a finished diameter of 0.250" was obtained. The electroform was cooled in liquid nitrogen and expanded into a close fitting hole in the brass body of the transformer -- see Fig. 5.3.

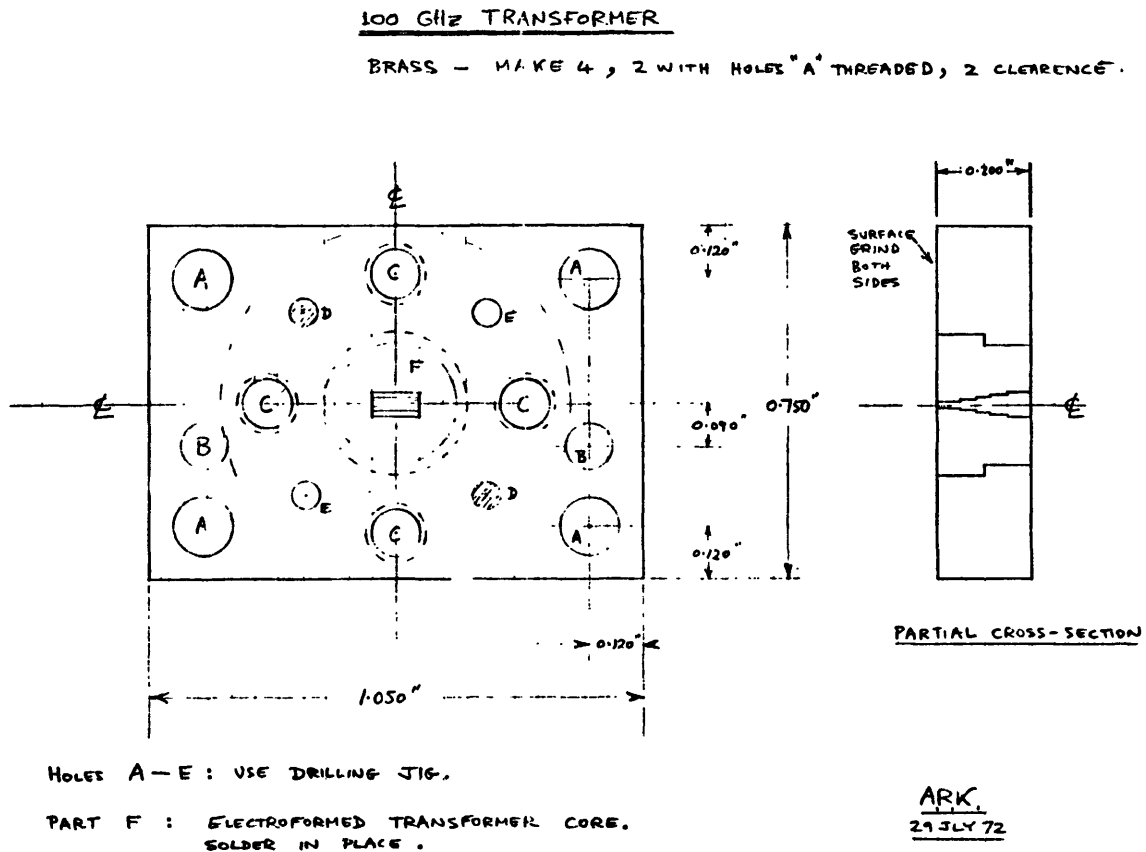


FIG 5.3

5.1.2 Diode Mount

The diode mount consists of two blocks, as shown in Fig. 5.4, bolted and pinned together. Relief is provided to ensure contact between the two parts along the waveguide wall. The blocks are separated to enable the diode chip to be soldered in place on the end of the RF choke.

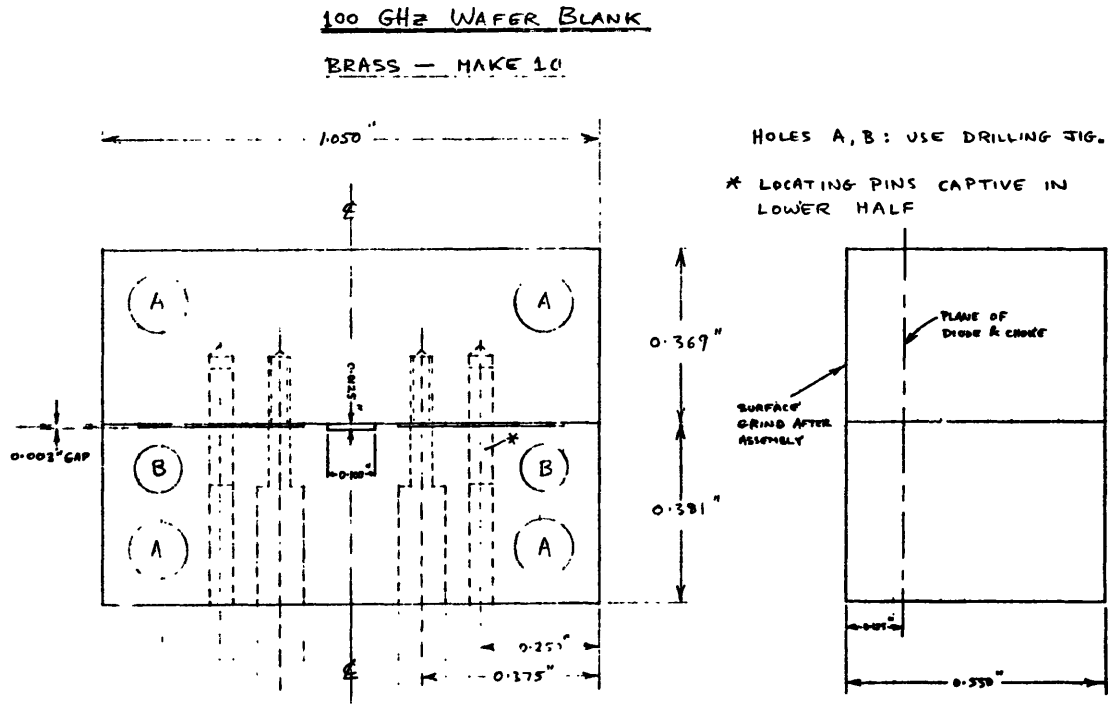


FIG 5.4

Details of the RF choke and its mounting are given in Figures 5.5 and 5.6. The computed frequency response is shown in Fig. 5.9. This is the impedance seen looking into the choke from the waveguide, assuming a 50 Ohm termination at the OSM connector. The dielectric loss tangent was assumed to be 0.002, the conductor resistivity 4 times that of copper, and the relative dielectric constant 1.8. Fringing capacitance at the steps was taken into account, but higher modes were assumed cutoff. (Cutoff for the TE_{11} on the high impedance sections of the choke is ~170 GHz.) If a practical useful frequency limit for the choke is taken to be when the real part of the choke impedance reaches 1 Ohm, or when the imaginary part reaches 10 Ohms, it is clear that this choke should operate satisfactorily from 60 to 150 GHz.

The RF choke is made from a single shaft of beryllium copper with two brass sliders (0.0208" diameter) which are soldered in place. The choke is gold plated after assembly, and then four 0.003" diameter spherical glass beads* are epoxied on each of the sliders, at 90° spacing. These center the choke in the 0.027" diameter tube during curing of the Stycast.

Considerable care must be taken in using the Stycast dielectric material. Stycast 36-DD** was used for the original mounts, but this is no longer available, and Stycast 35-D has been used recently, mixed with Eccospheres FTF-15*** to achieve a fluid in which the spheres are nearly close packed. The resulting relative dielectric constant is estimated to be ~1.8. Stycast 35-D will not

* Selected from commercial sandblasting beads -- "Trinbeads"

** Emerson-Cuming Co.

*** Eccospheres FTF-15, from Emerson Cuming, are SiO_2 balloons of diameter < 40 microns, and wall thickness < 1 micron. Cost in Jan. 1973, \$50 per lb. Stycast 35-DS was not used since the maximum size of its spheres was ~125 microns (≈0.005") which is too large to fill the choke recesses.

100 GHz CHOKE

MAKE 5

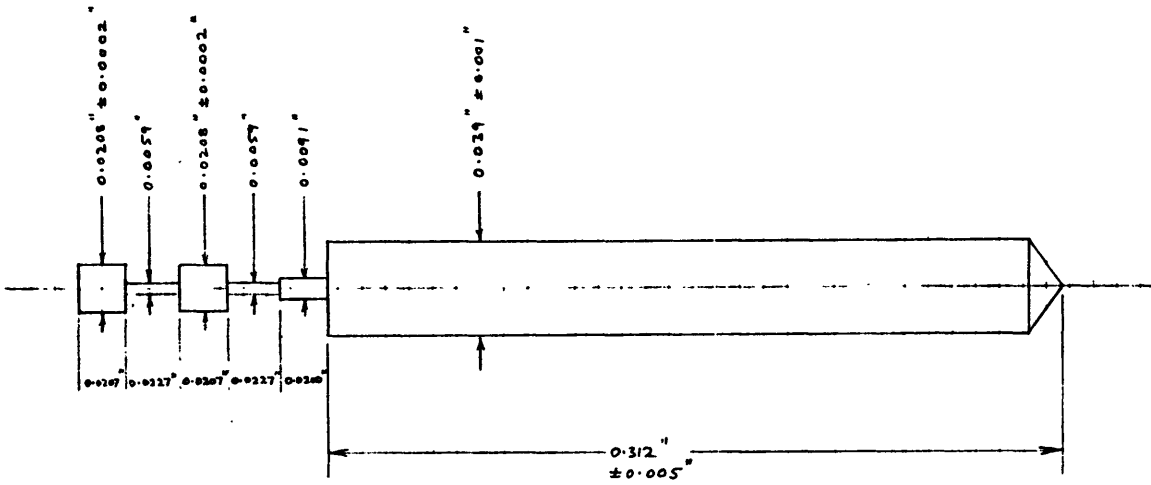


FIG 5.5

TOLERANCE ± 0.0004"
UNLESS INDICATED.

A.R.K.
30 JULY 72

DETAILS OF 100 GHz CHOKE & WAFER INSERT

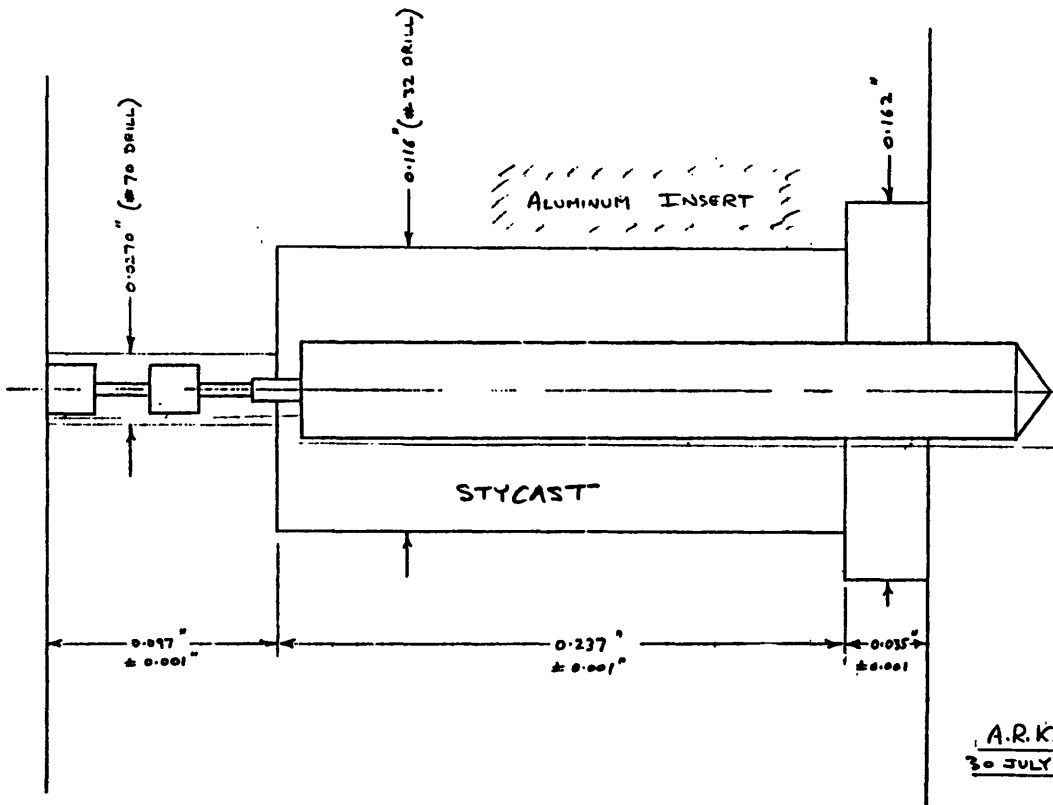


FIG 5.6

A.R.K.
30 JULY 72

cure satisfactorily against a copper-bearing metal due to a chemical reaction with the copper, and for this reason it is important that (i) the choke be well gold plated, (ii) an insert of aluminum be inserted in the appropriate block of the mount (or, alternatively, the mount could be made of aluminum). Our technique for "injecting" the Stycast was to fill the choke mounting hole with Stycast, and then to gently insert the choke, letting it sink gradually to a stop at the bottom of the small diameter hole. A reservoir of Stycast was provided each end of the hole to allow for the evolution of air trapped during mixing; air bubbles from the choke region are thus replaced by Stycast as they rise to the surface. Excess Stycast is chipped and scraped away after curing.

The diode chip is attached to the end of the choke using low temperature solder (e.g., Alpha 20E2 96 °C melting point). The choke should be thermally connected to the block (at the connector end) and the whole assembly carefully heated to avoid overheating the Stycast or the chip above ~150 °C.

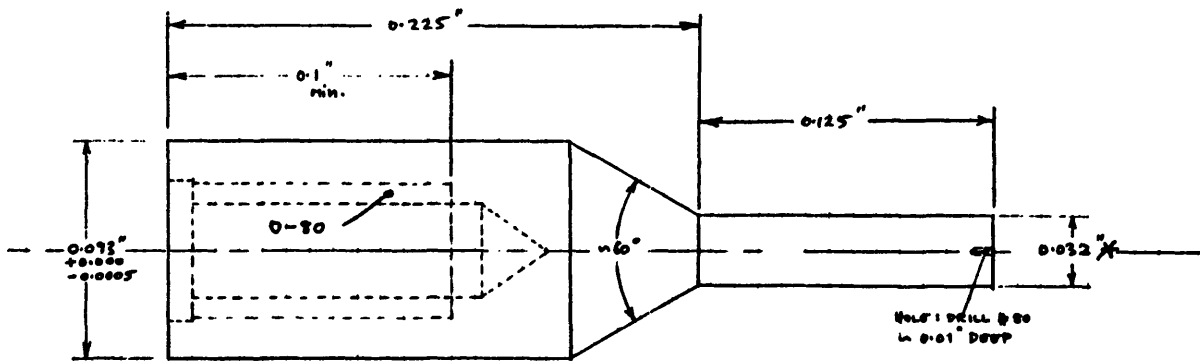
The lower block of the mount is drilled to receive the copper whisker-pin (Fig. 5.7). The whisker is soldered into the #80 hole in the tip of the pin. The pin should be slightly tapered to ensure a firm fit at the tip where it enters the waveguide. Old pins that are too loose can be finely knurled by rolling the tip along a fine file.

Several methods have been used for connecting the OSM connector to the RF choke. It was found that mechanical flexibility was necessary to prevent a small amount of movement being transmitted to the diode when a connector was mated with the mount. A short gold strap was found satisfactory (provided no soldering flux residue was left), and also a spring contact using a miniature gold plated nickel bellows.*

* Made by Servometer Corporation.

WHISKER PINS

MAKE 50 : SOFT COPPER



* 0.032" TO BE A TIGHT FIT IN HOLES ON TIG SUPPLIED.
THE TIGHT FIT IS MOST IMPORTANT AT THE TIP - DO
NOT ROUND ITS EDGES

A. R. KERR
13 AUG 72
PHONE: 296-0335

FIG 5.7

Alignment between the mixer-block and transformer was ensured by making a steel drilling jig. This plugs into the reduced height waveguide and contains all the holes shown in Fig. 5.3. Details of the jig are listed in Fig. 5.8.

DRILLING JIG FOR 100 GHz MOUNT

STEEL - MAKE 1

HOLE PATTERN AS FOR 100 GHz TRANSFORMER

TONGUE TO FIT 0.100" X 0.0125" WAVEGUIDE, SHOULD PROJECT BOTH SIDES.

SCREW HOLES (A & C) SHOULD BE TAPPING SIZE.

PIN HOLES (B, D, & E) SHOULD BE INTERFERENCE SIZE.

HOLES C, D, & E ARE STANDARD UG-387/U PATTERN.

SEE FIGURE FOR 100 GHz TRANSFORMER

ARK
29-JULY-72

FIG 5.8

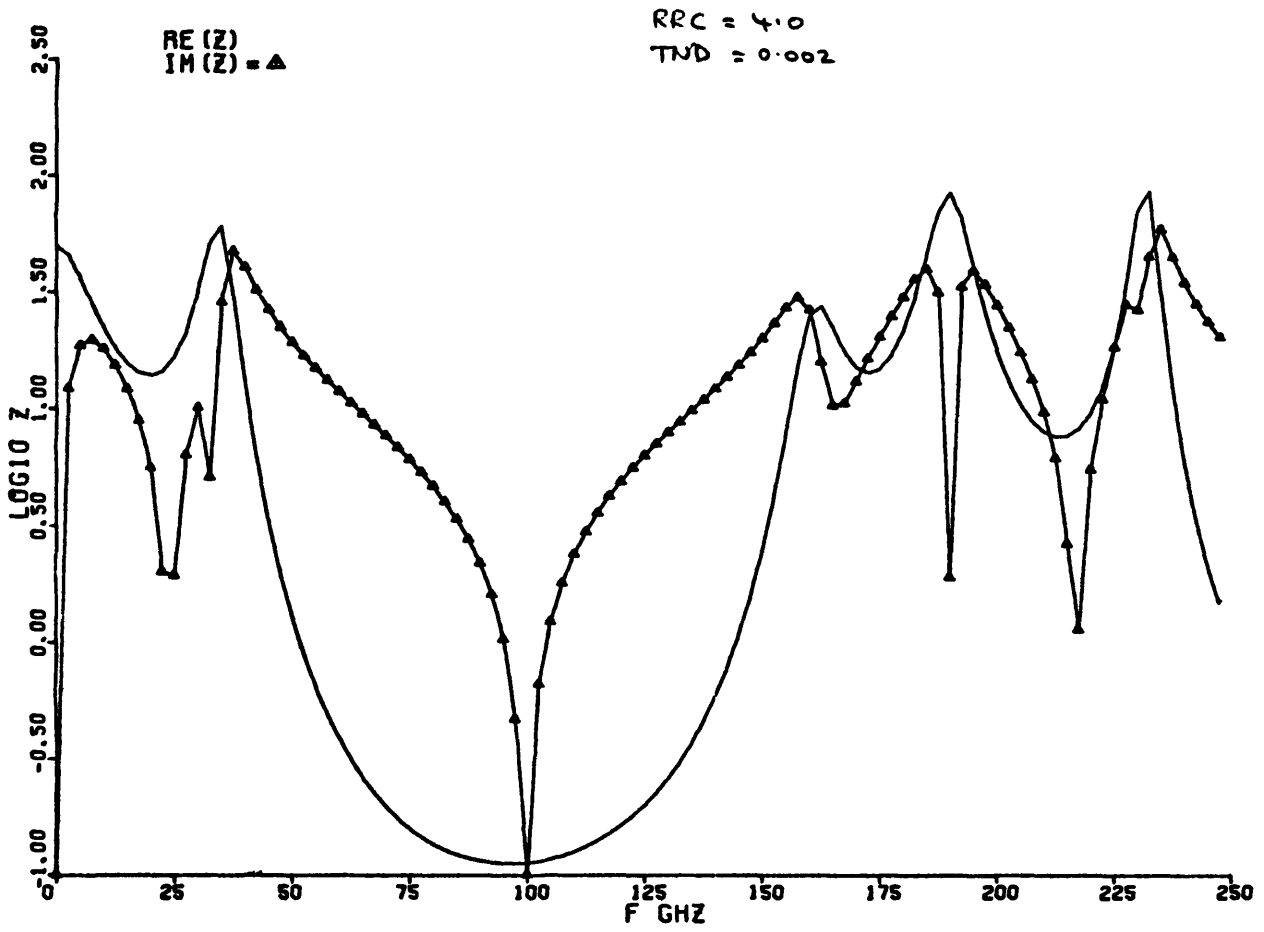


FIG 5.9

5.1.3 Backshort

The backshort was machined from a single piece of beryllium copper sheet. A thinned-down (to 0.002") slitting saw was used to mill a slot across the end of the short, and then to separate the fingers: see Fig. 5.10.

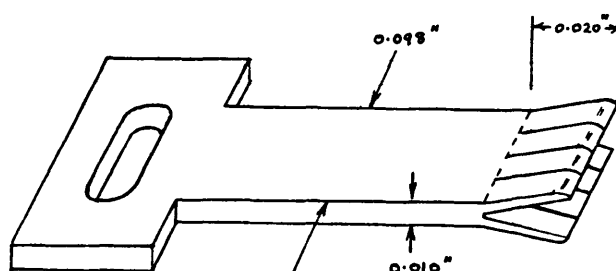


FIG 5-10

A fine stone was used to round the ends of fingers to facilitate insertion into the waveguide and to reduce mechanical scraping as the short is moved. The fingers were then spread using a knife blade, and the whole backshort heavily gold plated to increase the useful lifetime of the contact points.

The shoulder at the rear of the backshort is to prevent it from being pushed into the diode.

5.1.4 Performance

The table below gives the best results we have repeatedly measured for different diodes and frequencies. The measurements were made with the noise measuring test set described in Section 4.1. This is essentially a direct reading radiometer at the IF frequency, 1.4 GHz, with a built-in noise

reflectometer for measuring the IF-port mismatch of the mixer. Results obtained this way have been in good agreement with measurements using the conventional Y-factor method, and there is the added convenience that the IF-port need not be matched during the measurement.

Frequency	85 GHz		115 GHz	
Diode	3.5 μ	2.5 μ	3.5 μ	2.5 μ
L_{SSB}	6.2 dB	4.6 dB	6.7 dB	5.5 dB
$T_{MXR_{SSB}}$	700 °K	420 °K	1400 °K	500 °K
Bias V	0.6 V	0.4 V	0.4 V	0.4 V
Bias mA	4.0 mA	2.0 mA	4.0 mA	2.0 mA

5.2 A Cryogenic 3 mm Mixer

It was found that the room temperature mixer described above, could not reliably be cryogenically cooled. Differential contraction of the Stycast dielectric caused movement of the RF choke, and in many cases the diode would open circuit or change its characteristics. To overcome this a diode package was developed in which the RF choke, Ga As chip, and contact-whisker were all attached to a single strip of quartz supported across the waveguide; see Fig. 5.11. The whole diode structure was free to expand and contract within the brass mount, electrical contact being maintained by spring pressure. Electrically the cryogenic mixer is similar to the room temperature design, the main differences being:

- 1) the strip of quartz across the waveguide at the plane of the diode;
- 2) the RF choke is a printed circuit on the quartz structure;
- 3) the contact-whisker is not grounded directly through the waveguide

floor, but through a second RF choke.

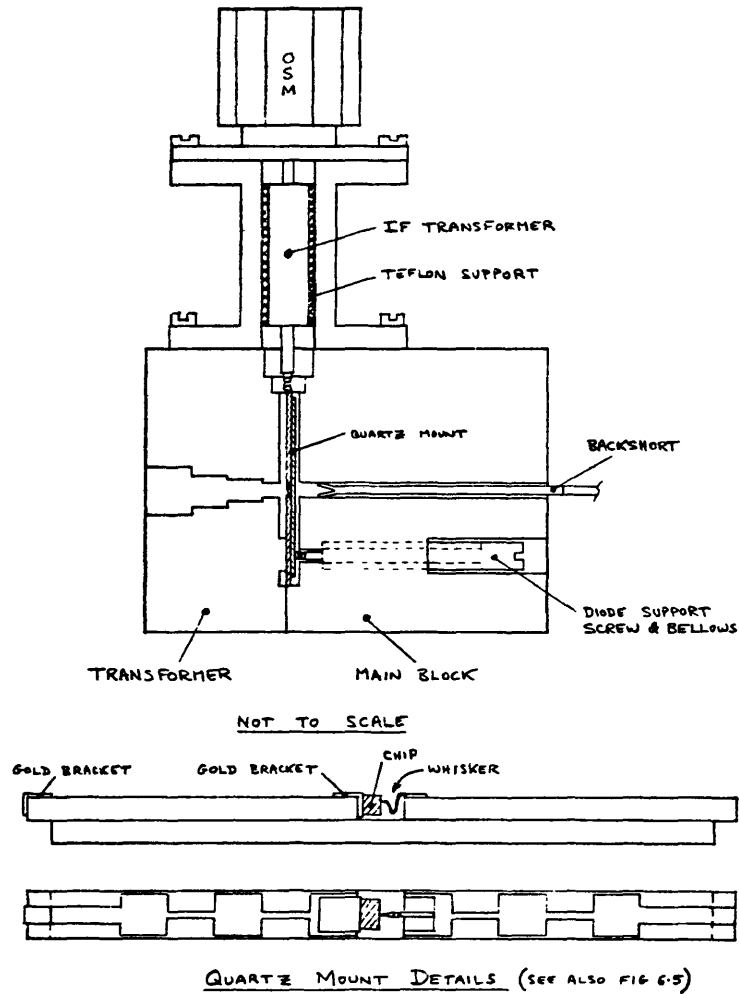


FIG 5-11

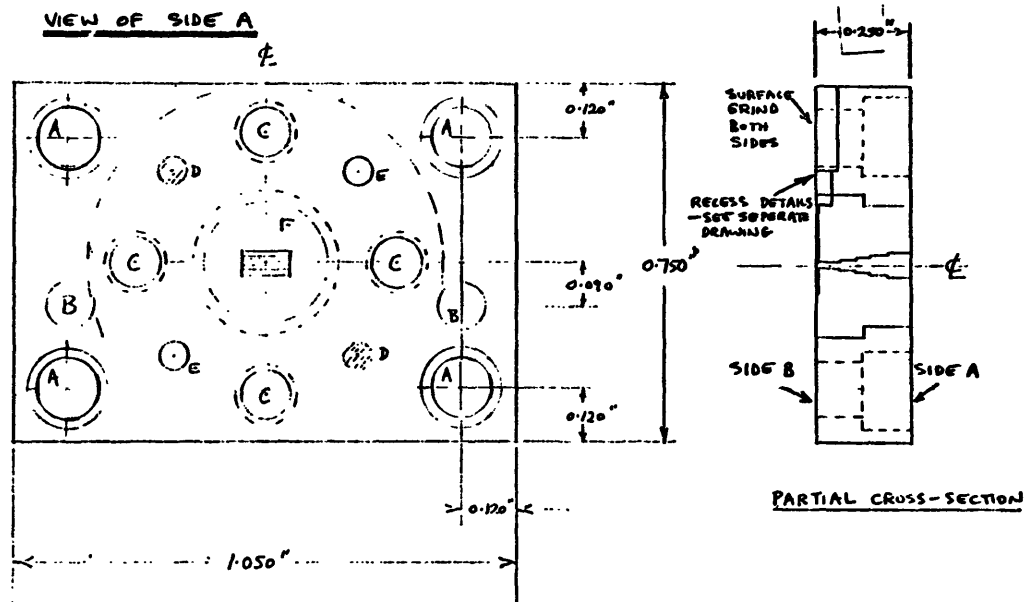
5.2.1 Waveguide Transformer

The waveguide height-reducing (4:1) transformer is essentially the same as the one described in Section 5.1.1 for the room temperature mixer,

except for some milling to provide clearance for the diode which is supported between the transformer and the main block. Details of the waveguide transformer and the milling are given in Figures 5.12 - 5.14. Construction details are described in Section 5.1.1.

QUARTZ MOUNT - TRANSFORMER SECTION

DRWG. -- MAXC 1



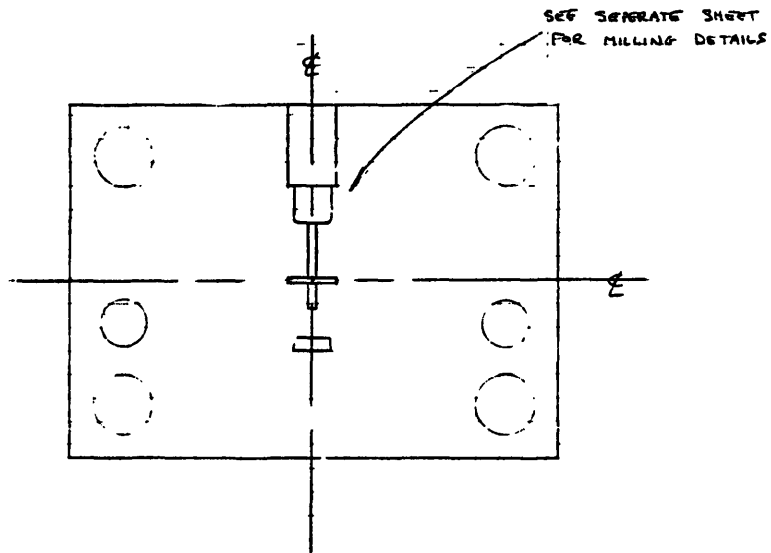
Holes A-E : USE DRILLING JIG.
Hole A : # 4 CLEARANCE AND RECESSES FOR SCREW HEADS
PART F : ELECTROFORMED TRANSFORMER CORE.

ARK
18 OCT 73
PROJ # 2.576

FIG 5.12

QUARTZ MOUNT — TRANSFORMER SECTION

VIEW OF SIDE B



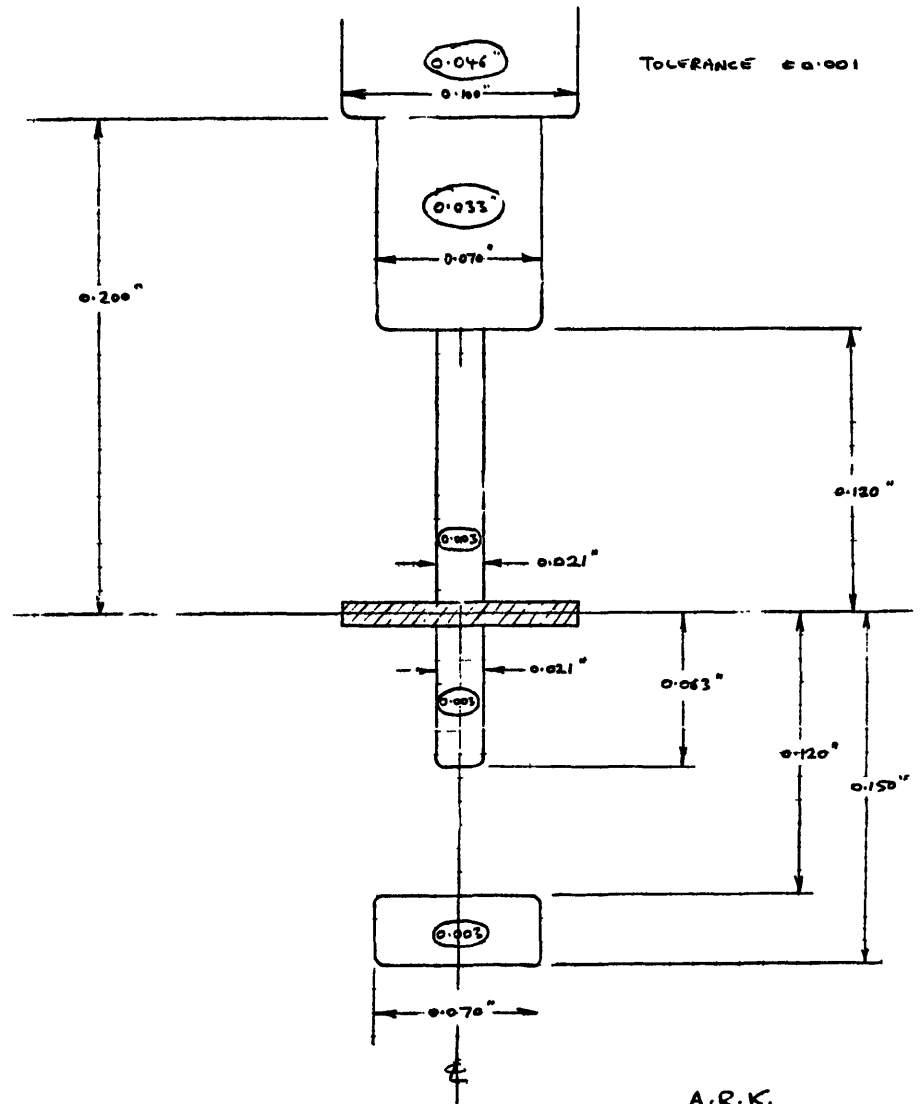
ARK

18 OCT 73

PROJ. # 2-576

FIG 5.13

MILLING DETAIL FOR QUARTZ MOUNT HOLDER (TRANSFORMER SECTION)



A.R.K.
PROJ. # 2-576
18 OCT 73

FIG 5.14

5.2.2 Main Block

The main block is a section of 1/4 - height waveguide with a milled recess to hold the diode. The waveguide section is electroformed on an aluminum mandrel and then inserted into the brass body after cooling in liquid nitrogen. The diode support screw pushes a miniature bellows spring against the rear quartz surface of the diode and maintains contact between the lower choke section and the face of the waveguide transformer section; this ensures a DC return path.

Drawings of the block are given in Figures 5.15 and 5.16.

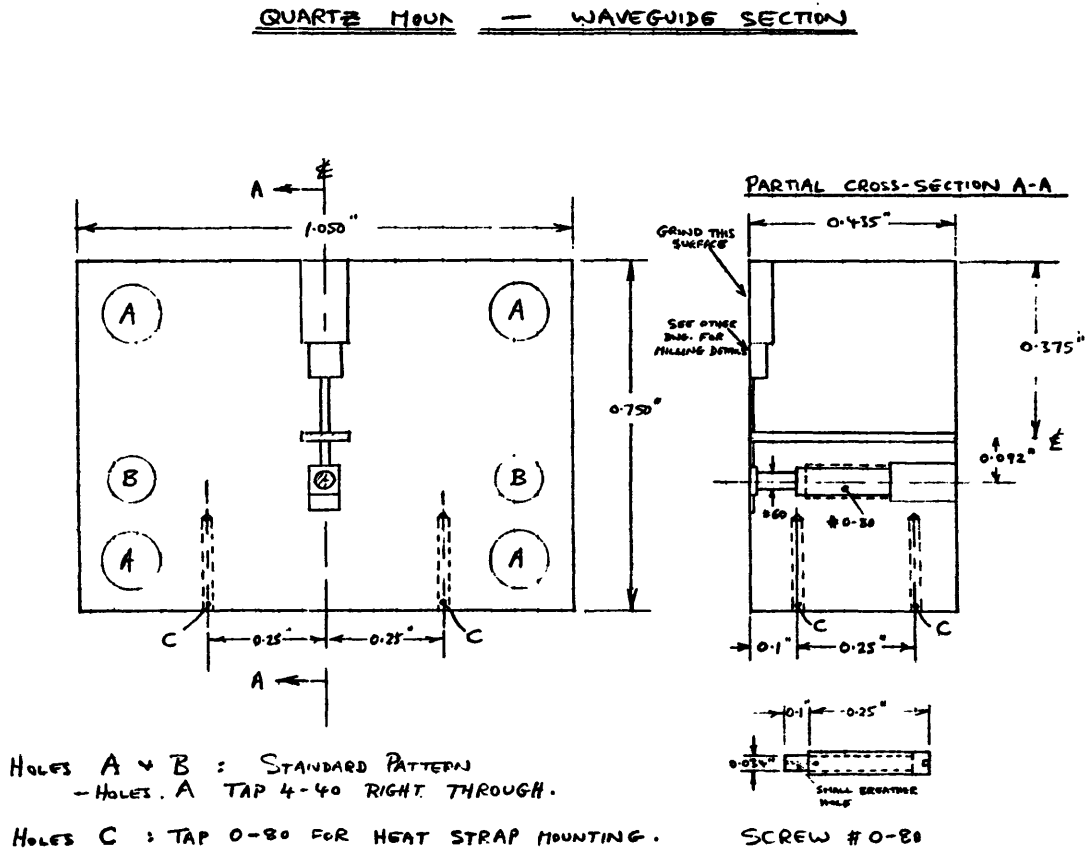
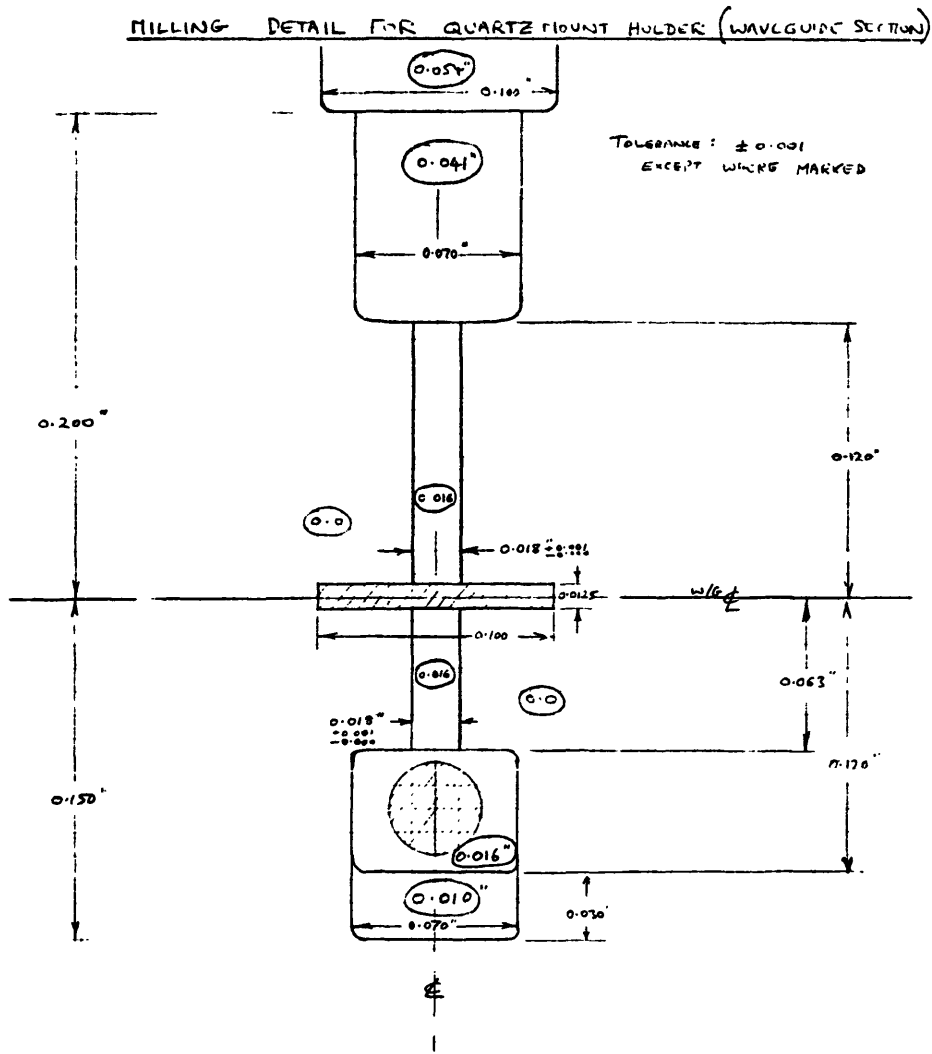


FIG 5.15

A.R.K.
 PROJ. # 2-576
 18 OCT 73



A.R.K.
PROJ # 2-576
18 OCT 73

FIG 5.16

5.2.3 Backshort and Drive

The backshort is identical to that described in Section 5.1.3.

A special micrometer drive was designed for cryogenic operation without excessive backlash; it is shown in Fig. 1.17. The micrometer screw and nut are modified from a standard 1/2 inch micrometer; both are steel. Differential expansion between the brass body and the steel micrometer parts is taken up by the spring washer against the ball bearings.

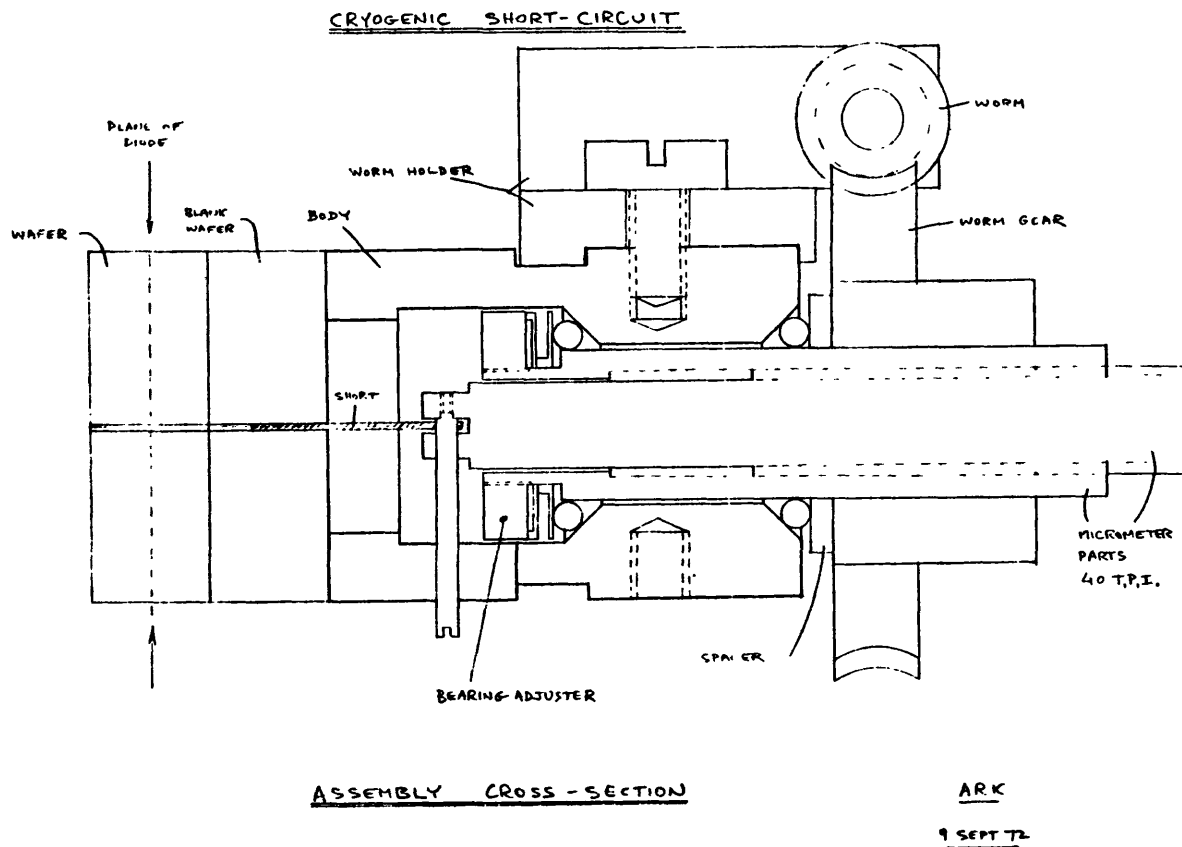
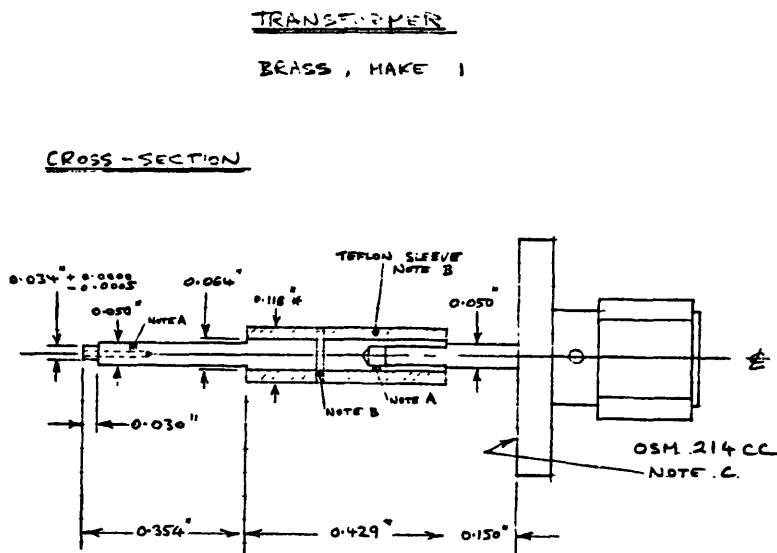


FIG 5.17

5.2.4 IF Transformer

The IF transformer consists of a quarter-wave section of 250 Ohm characteristic impedance coaxial line supported in a tight-fitting PTFE sleeve. A spring bellows contact* and a gold leaf spring make contact to the top of the diode. The transformer components are shown in Figures 5.18 and 5.19.



- NOTES: A- BREATHER HOLE (AS BEFORE) FOR SOLDERING.
- B- DOWEL OF TEFLON OR REXOLITE 0.020" DIAM. TO RETAIN TEFLON SLEEVE. ALTERNATIVELY: THE TEFLON SLEEVE MAY BE A TIGHT FIT, SUFFICIENT TO KEEP IT IN PLACE WHEN INSERTED INTO TRANSFORMER BODY.
- THE TRANSFORMER MUST BE A SMOOTH SLIDING FIT IN THE BODY
- C- THE FACE OF THE OSM CONNECTOR SHOULD BE MACHINED FLAT.

ARK
9 DEC 73
PROJ# 2.576

FIG 5.18

* Servometer Corp. Model 2510

TRANSFORMER BODY

BRASS, MAKE 9

A.R.K.
8 DEC 73
PROJ.# 2-576

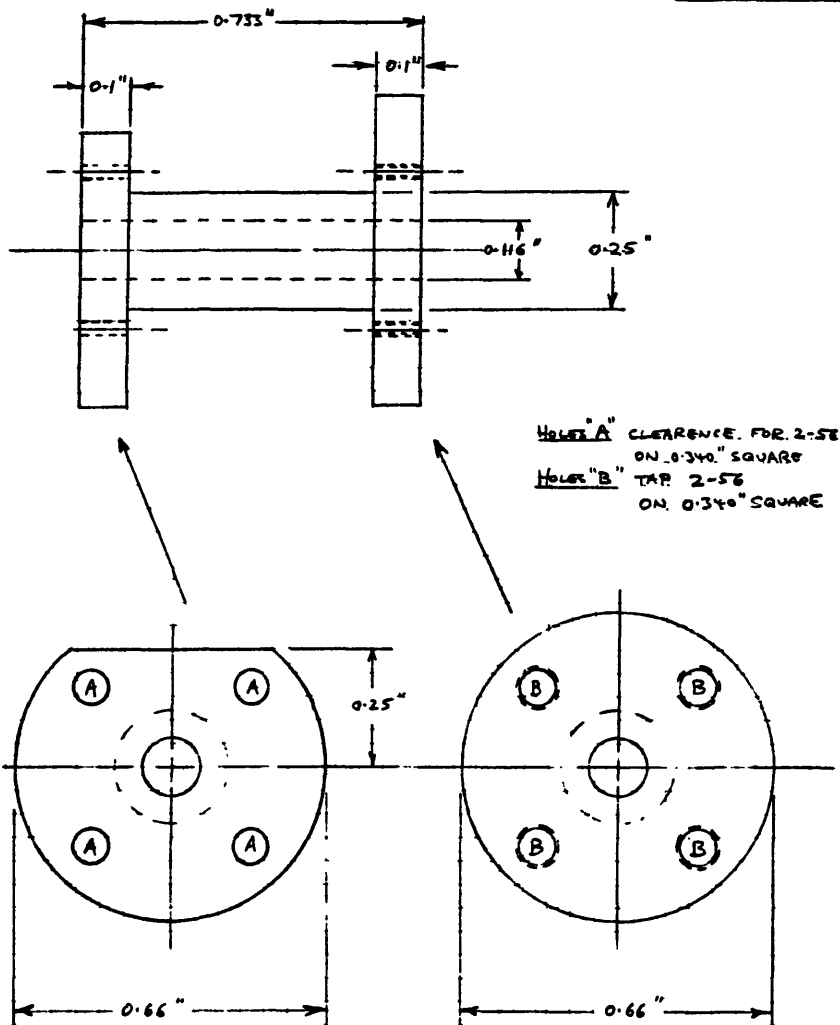


FIG 5.19

Details of the bellows and gold leaf spring are shown in Fig. 5.20.

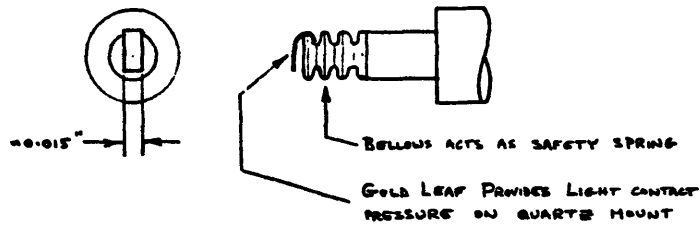


FIG 5.20

5.2.5 Performance

The mixer performance of the quartz-mounted diodes is summarized below for typical good diodes. The performance of diodes at 18 °K and at 77 °K was found to be essentially the same, and most testing was therefore done at 77 °K. Mixers operated with an IF of 4.75 GHz generally had about

RF FREQ. GHz	TEMP. °K	IF FREQ. GHz	L _{SSB} dB	T _{MXR} _{SSB} °K
115	298	1.4	5.4	740
115	77	4.75	5.8	300

0.2-0.5 dB worse conversion loss than with 1.4 GHz IF, and 5 to 10% higher T_{MXR}. This is believed to be due to higher IF matching circuit loss and to the poorer

RF match when the sidebands are separated by 10% of the RF frequency (with the 4.75 GHz IF), compared with 3% of the RF frequency with the 1.4 GHz IF.

6. DIODE FABRICATION AND CONTACTING

6.1 Diodes

The diode chips used in the mixers described in this report were all made by Dr. Robert Mattauch of the Department of Electrical Engineering at the University of Virginia. They are Schottky barrier diodes formed on epitaxial gallium arsenide by electroplating a platinum anode followed by gold. The specifications of the gallium arsenide are:

Epitaxial Layer:

Doping $3 \times 10^{17} \text{ cm}^{-3}$
 Thickness $0.5 \pm 0.25 \text{ micron}$

Substrate:

Orientation (100)
 Type n
 Doping $2 - 3 \times 10^{18} \text{ cm}^{-3}$

Typical diode characteristics, measured at DC and room temperature, are given below:

DIODE DIAMETER	3.5 μ	2.5 μ
η	1.10	1.11
R_s	3.6 Ω	8.0 Ω
$C_{j_{ov}}$	0.030 pF	0.007 pF
$f_c = \frac{1}{2\pi R_s C_{j_{ov}}}$	1500 GHz	2800 GHz

The parameters η and R_s are defined by the diode equations

$$I = I_o \left(e^{\frac{qV'}{\eta kT}} - 1 \right) \quad (6.1)$$

$$V' = V - I R_s \quad (6.2)$$

A plot of $\log I$ vs. V yields these parameters as shown in Fig. 6.1.

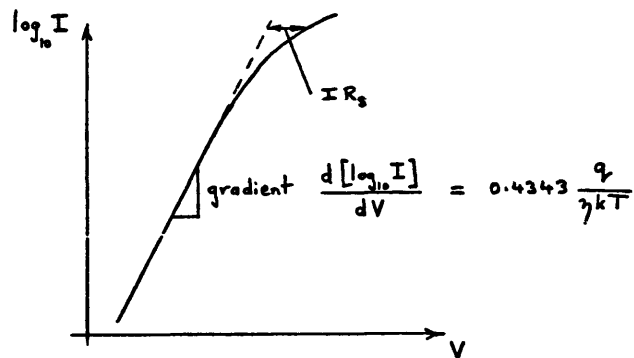


FIG 6.1

Capacitance values were measured at 1 MHz using a Boonton model 75 bridge. $C_{j_{ov}}$ is the diode junction capacitance at zero bias.

6.2 Contact Whiskers

The contact whiskers on all the mixers described here are made from 0.0005" diameter phosphor bronze wire, electrolytically pointed, then gold plated. The point diameter was made somewhat smaller than the diode diameter in order to reduce the stray capacitance between the whisker and the GaAs chip. Typical whisker tip diameters were 1/2 to 3/4 of the diode diameter.

During the whiskering of a diode great care was taken to ensure that the whisker entered directly into the diode and was not damaged by sliding between diodes on the SiO_2 surface of the chip. Experience has shown that although diodes formed with damaged whiskers may have good DC characteristics (η and R_s), they usually have high conversion loss (up to 2 dB worse than normal) because of the excess capacitance between whisker and chip.

6.2.1 Diode Contacting -- Room Temperature Mixers

The configuration of the room temperature mixers was such that it was not possible to watch the whisker point entering a particular diode dot, but only to look straight down the waveguide and watch the whisker approaching the chip. A capacitance bridge^{*} was used to monitor the capacitance between the whisker and the diode as the whisker was advanced; a typical plot of C vs. x is shown in Fig. 6.2. Section A-B of the curve shows the increasing capacitance between whisker and chip as the whisker is advanced. When contact is made a sudden jump, B-C, is seen, equal to the capacitance of the diode. Further advancement deforms the whisker tip, resulting in excessive shunt capacitance around the diode -- curve section C-D. With a little practice it is possible to determine from section A-B of the curve,

* Boonton Model 75.

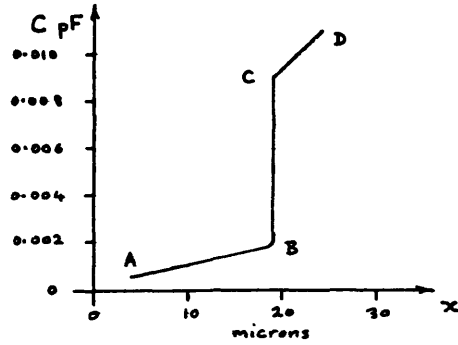


FIG 6.2

whether the whisker has hit directly on a diode or has become deformed by hitting the SiO_2 surface of the chip.

A total whisker length of 0.005" to 0.006" was used on the room temperature mixers. A spring was formed (Fig. 6.3) using a hand-held scalpel blade while the whisker was positioned against a ground steel edge using a micro-manipulator.

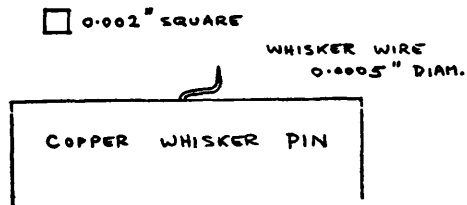


FIG 6.3

6.2.2 Diode Contacting -- Cryogenic Mixers

In the case of the quartz diode mounts the diode chip was able to be obliquely illuminated through the quartz, and viewed from an appropriate direction using a long focal length high magnification microscope. It was thus possible to watch the whisker approaching the chip and to determine whether it would hit one of the Schottky dots. A curve tracer oscilloscope monitored the I-V characteristic to determine the initial contact between whisker and diode. For the cryogenic mixers described below, the whisker was pushed a further ~1.2 microns beyond initial contact; this was found to give sufficient spring compression to take up differential contraction between the whisker and the quartz structure on cooling, while not damaging the diode. It was found that with a little too much whisker pressure the whisker would gradually work its way through the metal contact on the diode. This would be accelerated by repeated temperature cycling, and was seen as a softening of the "knee" of the I-V characteristic as the whisker material came into direct contact with the surface of the gallium arsenide and formed, in effect, a point contact diode in shunt with the original Schottky diode.

The whisker shape is shown in Fig. 6.4. The total length of wire in the whisker was 0.008" to 0.009", a compromise between best conversion loss with

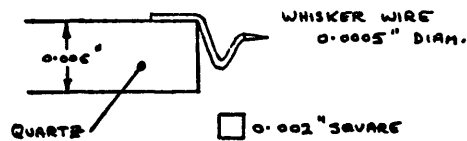


FIG 6.4

a shorter whisker, and reliability due to the better spring characteristics of the longer one. The whisker bending technique is described in Section 6.3.5.

6.3 Fabrication of the Quartz Diode Mounts

To overcome the differential contraction between the dielectric material supporting the RF choke, and the metal body of the mixer, the diode chip and contact whisker were supported by a structure made of a single dielectric material. Fused quartz was chosen, not for its expansion coefficient (which is very low, and thus maximizes differential effects), but for its low dielectric constant (3.8) and loss tangent, and its high mechanical strength and rigidity. To allow differential expansion between the quartz and the metal body of the mixer, the whole quartz structure was supported in a slightly oversized channel in the body. The mounting details are shown in Fig. 5.11. Details of the diode are given in Fig. 6.5.

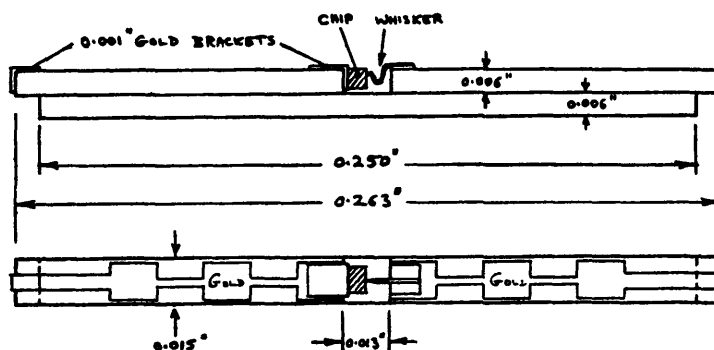


FIG 6-5

6.3.1 Photolithographic Choke Fabrication

Fused quartz pieces 0.7" x 0.7" x 0.006" were chrome-gold metallized on one side by Dr. Mattauach at the University of Virginia.* A thin chromium layer, necessary for good adhesion, is followed by a thicker gold layer (~0.5 micron). These were coated with resist, exposed, developed, baked, etched, and cleaned, as described in detail in Appendix 4. The final result was an array of 60 chokes on each 0.7" square quartz piece. These were separated by scribing and breaking the quartz as described in the following section.

6.3.2 Cutting the 0.006" Quartz

Since the fused quartz is amorphous, strictly a "glass," it is easily cut by scribing and breaking. A Kulicke & Soffa model 750** diamond wafer scribe was used for this. A stylus force of 50-60 grams was sufficient to cut through residual gold when necessary but did not give excessive chipping. To obtain a clean break along the scribe line a little operator practice is needed. Two pairs of #7 tweezers in new condition were used; to obtain a square cleavage along the full length of the scribe line it is necessary to avoid a shearing action between the two pieces, and maintain only a torsional force -- see Fig. 6.6.

* Materials Research Corp., and Valpey Corp. will also perform this operation with varying success rates.

** No longer manufactured.

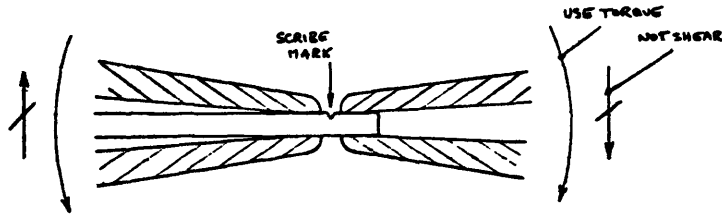


FIG 6-6

6.3.3 Bonding to the Quartz

Gold tabs are bonded to the metallized quartz to form the end contact, chip support bracket, and the whisker pad. Gold foil, 0.001" thick, was used, and bonded with an ultrasonic wire bonder using a 0.005" diameter tool to form a number of spot welds over the 0.015" square area to be bonded.

6.3.4 Mounting the Chip

The gallium arsenide chip was soldered to the gold support bracket using the Alpha 20E2 (96 °C M.P.) solder and Superior Supersafe 30 flux. A temperature controlled stage was maintained at 100-110 °C* while nitrogen gas was blown across the work area to slow down the build-up of scale on the molten solder. The chip was positioned centrally on the support

* Temperatures above ~150 °C have been found to permanently damage the diodes.

bracket using fine tweezers.

6.3.5 Mounting and Bending the Whisker

A pad of 0.001" gold was ultrasonically bonded to the end of the RF choke as described in Section 4.3.3. The pointed (but as yet unbent) whisker was laid in position on the gold pad using an X-Y-Z micropositioner, and ultrasonically bonded to the pad. Bonding between the phosphor-bronze whisker and the gold pad was not generally reliable, so the whisker was then soldered using the same procedure as described in Section 6.3.4.

To bend the whisker, a piece of 0.005" material was slid under the tip as a support, and a sharp (new) scalpel blade used to form the "V"-bend, leaving the point sticking up in the air. The point was then carefully bent over with the blade to form the desired shape -- Fig. 6.4.

6.3.6 Assembling the Three Quartz Pieces

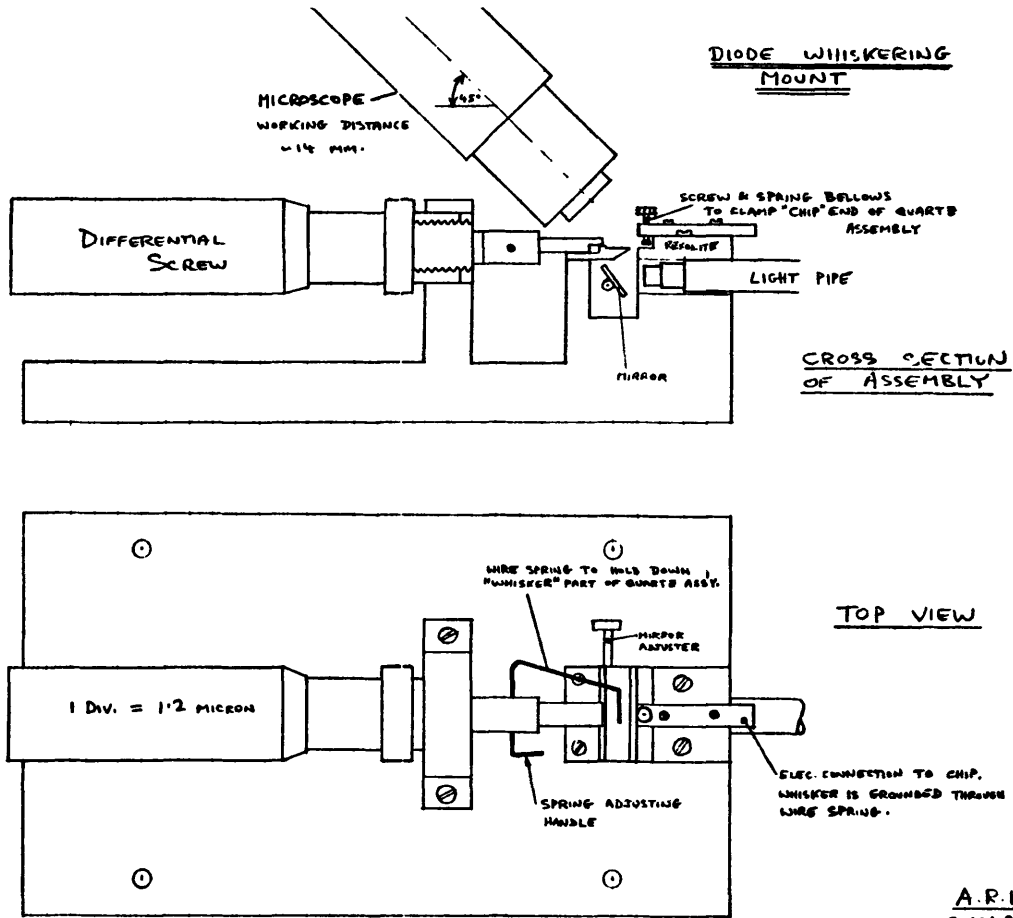
First the choke with a chip attached to it was positioned on top of the long backing piece, using a jig. Eastman 910 adhesive was applied to the line between the two quartz surfaces and allowed to run into the interface by capillary action. To prevent accidental adhesion between the quartz and jig, a mould release coating of fine PTFE particles* was applied to the jig in advance. Great care was necessary to ensure that no dust or PTFE particles were present between the surfaces to be glued, as the cyano-acrylate bond formation is only effective between surfaces in very close proximity. Moderate bond strength is developed in a few seconds, and the assembly can be removed

* Eccospray TFE-20 Emerson & Cuming, Canton, Mass.

from the jig and cleaned with Freon solvent to remove adhering PTFE particles.

This assembly was next mounted on another jig, also coated with mould-release agent. Electrical contact was made to the choke by a spring which also served to mechanically secure the assembly. The third quartz piece, with the contact whisker attached, was positioned on the long backing piece, and electrical contact made to it by a second spring. A differential micrometer screw* was used to advance the whisker towards the chip until contact with a diode was achieved -- see Section 4.2.2. Eastman 910 adhesive was applied to the interface of the quartz pieces. A sketch of the jig for contacting the diodes is given in Fig. 6.7.

* Model 22-505, Lansing Research Corp., Ithaca, N.Y. Total travel 0.050"; scale increment 0.00005" = 1.27 microns.



A.R.K.G.R.
18 MAR 73
2-475

FIG 6.7

7. REFERENCES

1. S. Weinreb, and A. R. Kerr, "Cryogenic Cooling of Mixers for Millimeter and Centimeter Wavelengths," IEEE J. Solid State Circuits, Vol. SC-8, No. 1, p. 58-63, Feb. 1973.
2. W. M. Sharpless, "Wafer-Type Millimeter Wave Rectifiers," BSTJ, p. 1385-1402, Nov. 1956.
3. S. A. Schelkunoff, "Electromagnetic Waves," Van Nostrand, 1943.
4. H. C. Torrey and C. A. Whitmer, "Crystal Rectifiers," M.I.T. Radiation - Lab. Series, Vol. 15, New York: McGraw Hill, 1948.
5. M. R. Barber, "Noise Figure and Conversion Loss of the Schottky Barrier Diode," IEEE Trans. Microwave Theory and Techniques, Vol. MTT-15, pp. 629-635, Nov. 1967.
6. D. A. Fleri and L. D. Cohen, "Nonlinear Analysis of the Schottky Barrier Mixer Diode," IEEE Trans Microwave Theory and Techniques, Vol. MTT-21, No. 1, p. 39-43, Jan. 1973.
7. A. A. M. Saleh, "Theory of Resistive Mixers," Ph.D. dissertation, M.I.T. Cambridge, Mass., 1970.
8. R. L. Eisenhart and P. J. Khan, "Theoretical and Experimental Analysis of a Waveguide Mounting Structure," IEEE Trans Microwave Theory and Techniques, Vol. MTT-19, No. 8, p. 706-719, Aug. 1971.
9. F. B. Hildebrand, "Advanced Calculus for Engineers," Prentice-Hall, N.J., 1948.
10. S. Egami, "Nonlinear, Linear Analysis and Computer-Aided Design of Resistive Mixers," IEEE Trans. Microwave Theory and Techniques, Vol. MTT-22, No. 3, p. 270-275, March 1974.
11. B. B. van Ipreu, "Impedance Relations in a Diode Waveguide Mount," IEEE Trans. Microwave Theory and Techniques, Vol. MTT-16, No. 11, pp. 961-963, Nov. 1968.
12. Y. Anand, "Noise-Factor Dependence on Mismatch of Low-Level R. F. Signal." Electronics Letters, Vol. 7, No. 4, p. 111-112, Feb. 1971.
13. G. L. Matthaei, L. Young, E. M. T. Jones, "Microwave Filters, Impedance-Matching Networks, and Coupling Structures, McGraw-Hill, New York, 1964.

APPENDIX 1: MOUNT MATCHING CURVES

The graphs give the real impedance (R_{sig}) of the mount as seen by the diode, and the corresponding shunt reactances (X_{SH}) of the backshort referred to the diode plane.

Z_g is the waveguide characteristic impedance as given by equation 2.1, and L is the lead inductance. The RF angular frequency is ω .

Solid curves are for R_{sig} , broken for X_{SH} .

Graphs are given for $\frac{1}{\omega C Z_g} = 5, 2, 1, 0.5, 0.2$ where C is the mean diode capacitance.

FIG. A1.1

$\frac{1}{\omega C Z_g} = 5.0$

AR.K.
15 Oct 71
MATCH 2

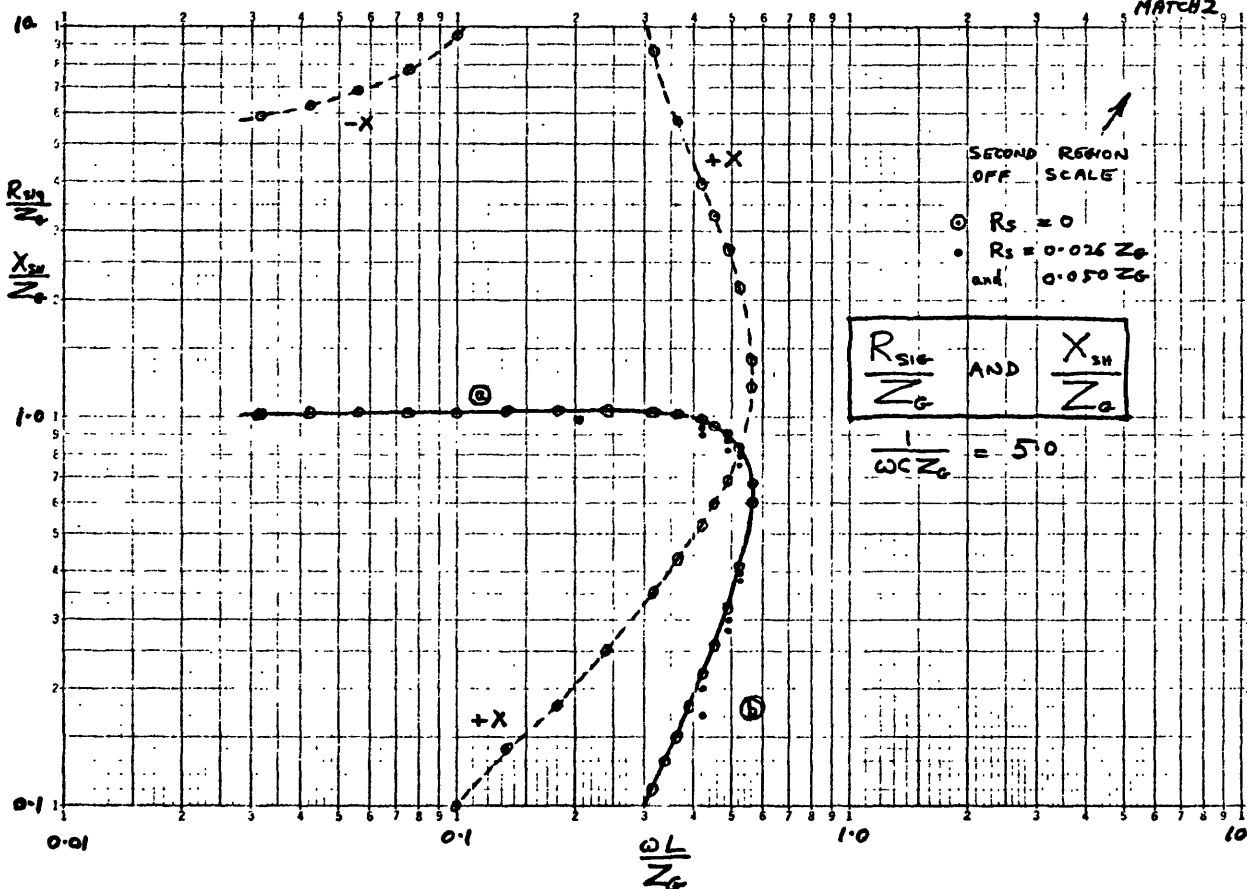


FIG. A1.2

$\frac{1}{\omega C Z_0} = 2.0$

A.R.K.
15 Oct 71
MATCH 2

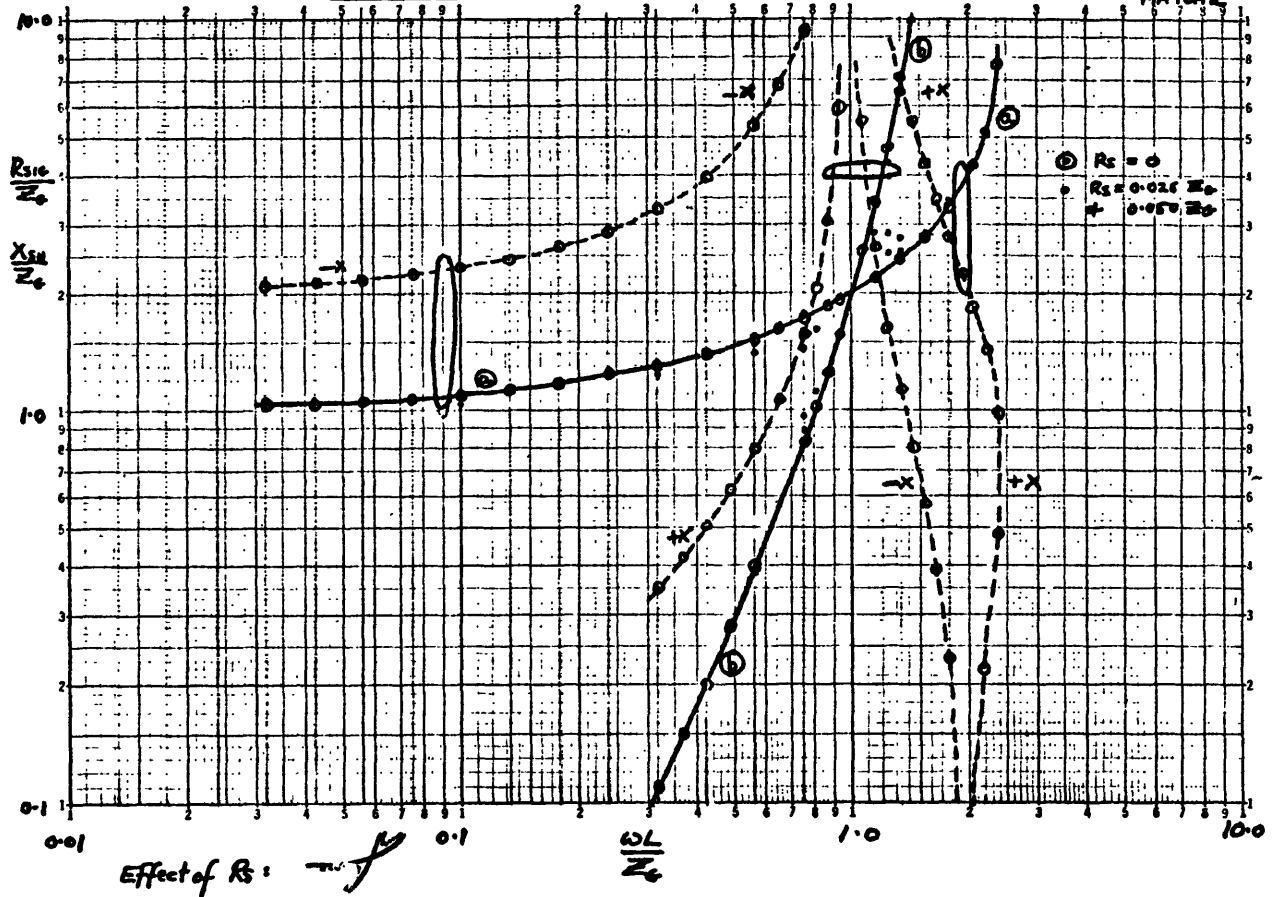


FIG. A1.3

$\frac{1}{\omega C Z_0} = 1.0$

A.R.K.
15 Oct 71
MATCH 2

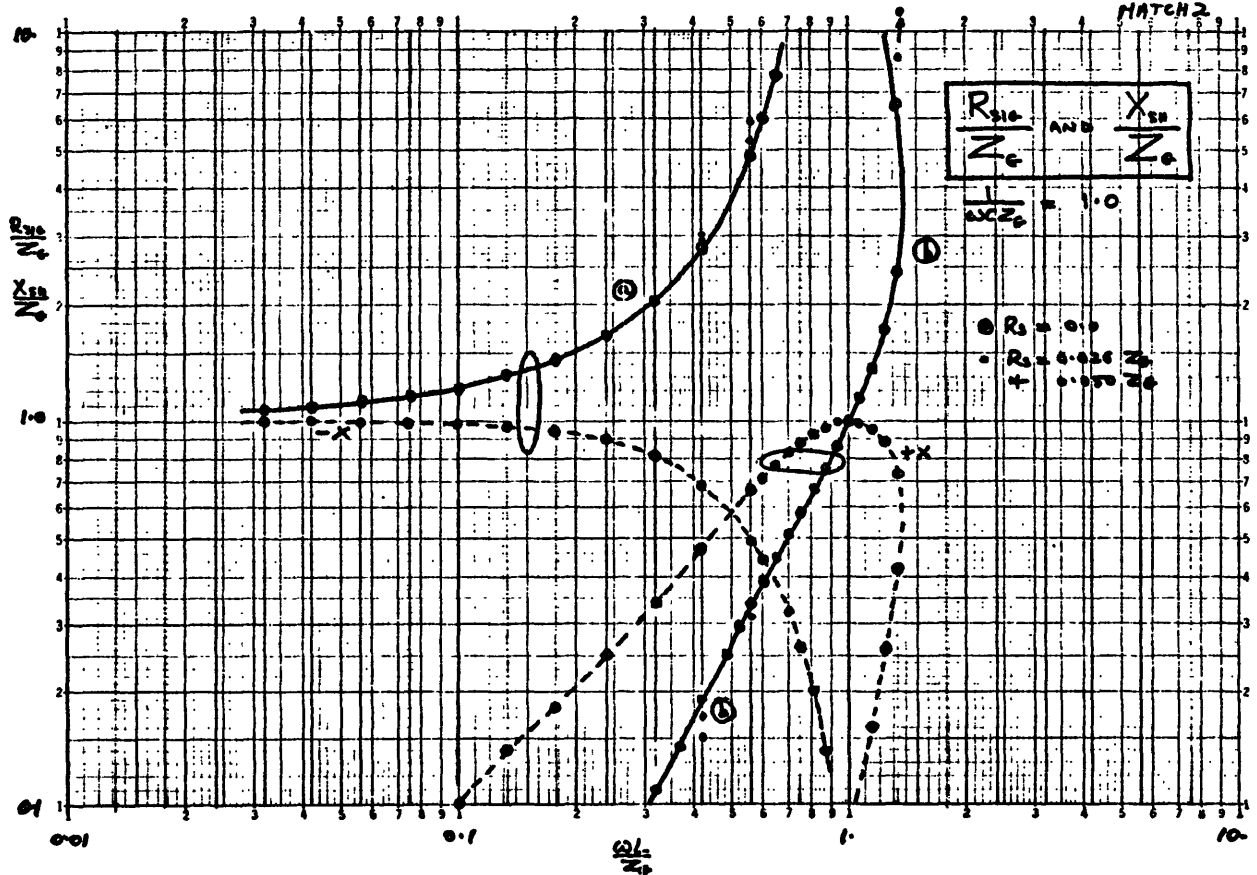


FIG. A1.4

$\frac{1}{\omega C Z_0} = 0.5$

A.R.K.
15 Oct 71
MATCH 2

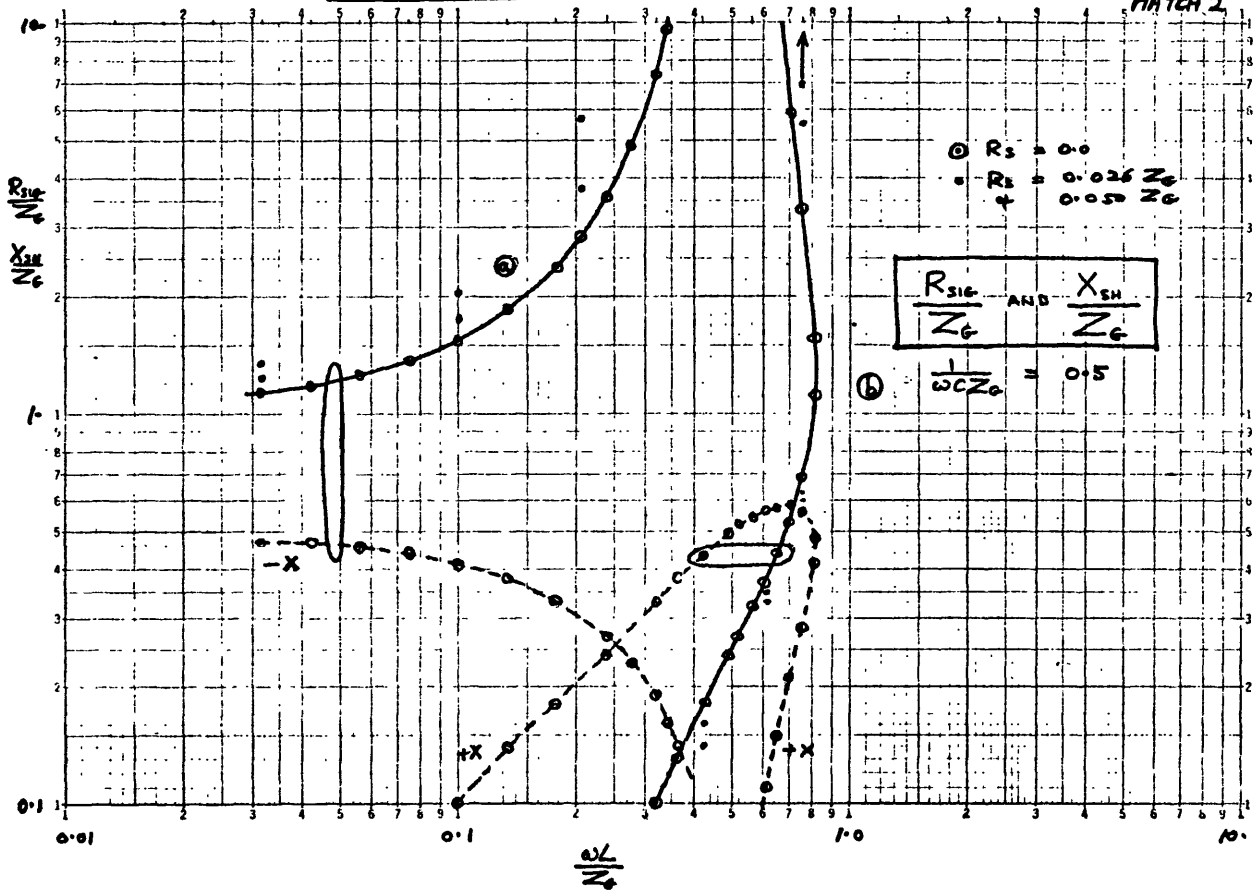
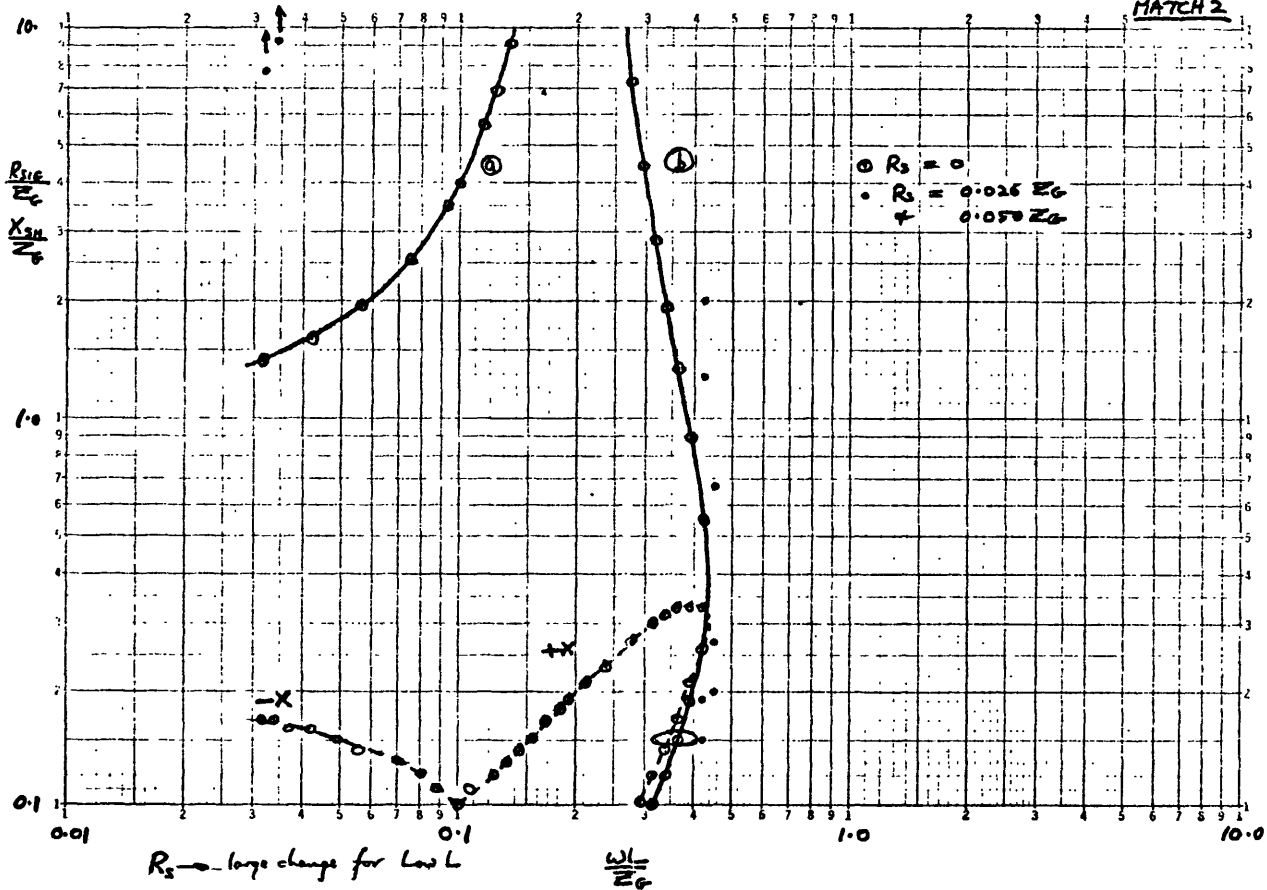


FIG. A1.5

$\frac{1}{\omega C Z_0} = 0.2$

ARK.
15 Oct 71
MATCH 2



APPENDIX 2: BANDWIDTH CURVES

These graphs give the 1 dB fractional bandwidth of the coupling of energy from the waveguide to the diode, when matched according to the graphs of Appendix 1: i.e., the diode resistance is assumed to be R_{sig} , and the back-short reactance at the diode plane is X_{SH} .

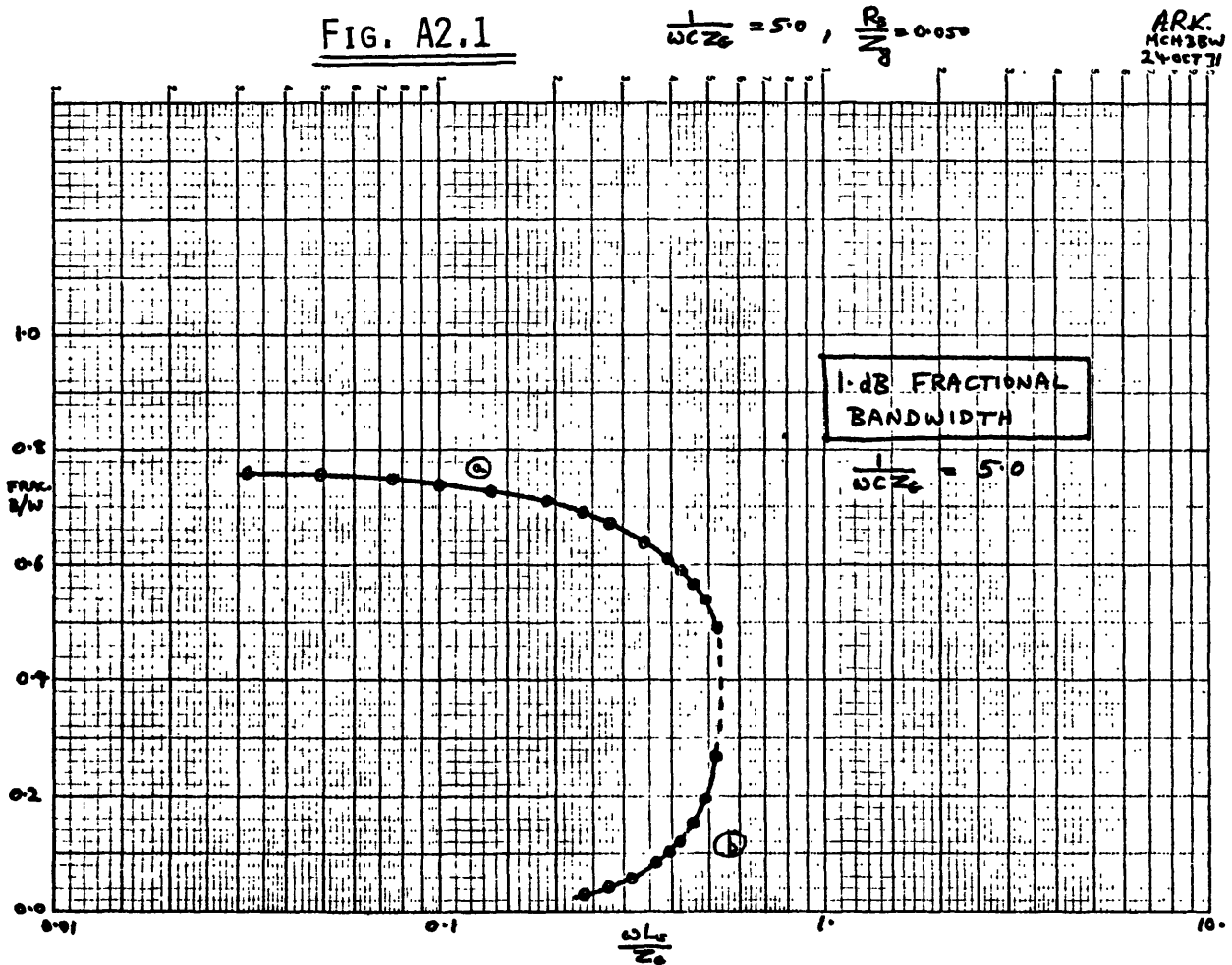


FIG. A2.2

$\frac{1}{\omega C Z_0} = 2.0$

ARK
MCM3BW
24 OCT 71

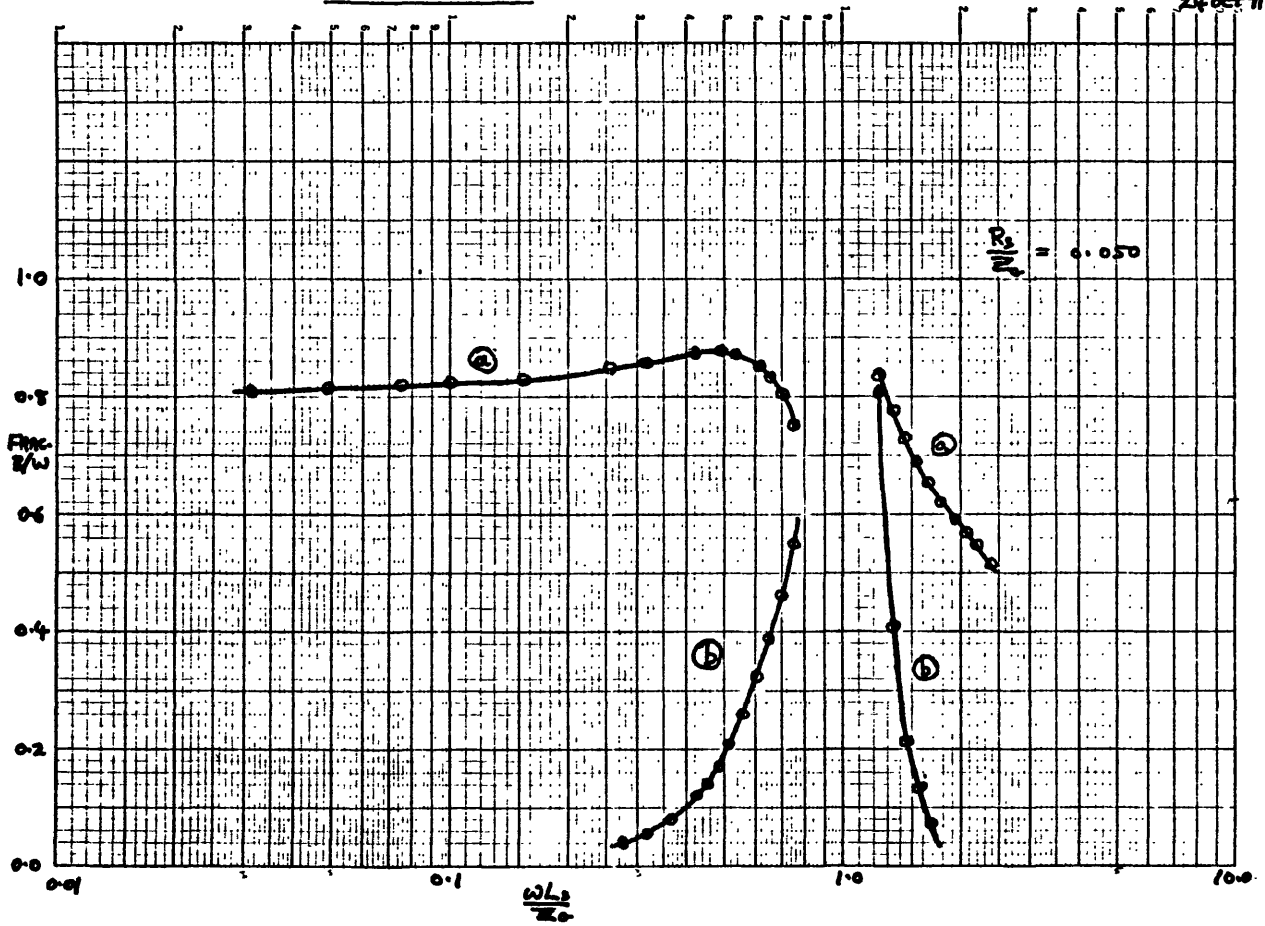


FIG. A2.3

$\frac{1}{\omega C Z_0} = 1.0, \frac{R_0}{Z_0} = 0.95$

ARK
MCM3BW
24 OCT 71

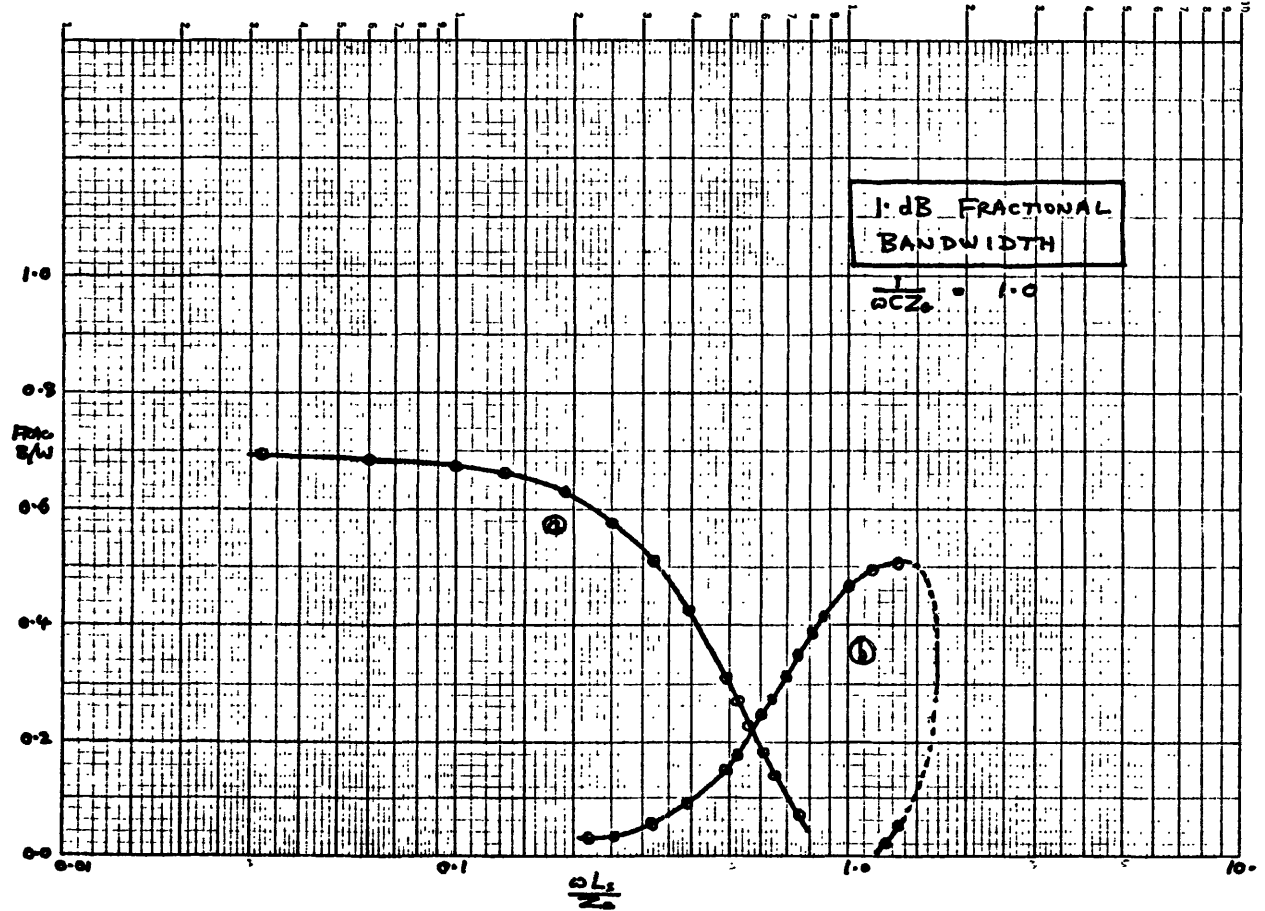


FIG. A2.4

$\frac{1}{\omega C Z_0} = 0.5, \frac{R_s}{Z_0} = 0.05$

A.R.K.
MCM38W
24 OCT 71

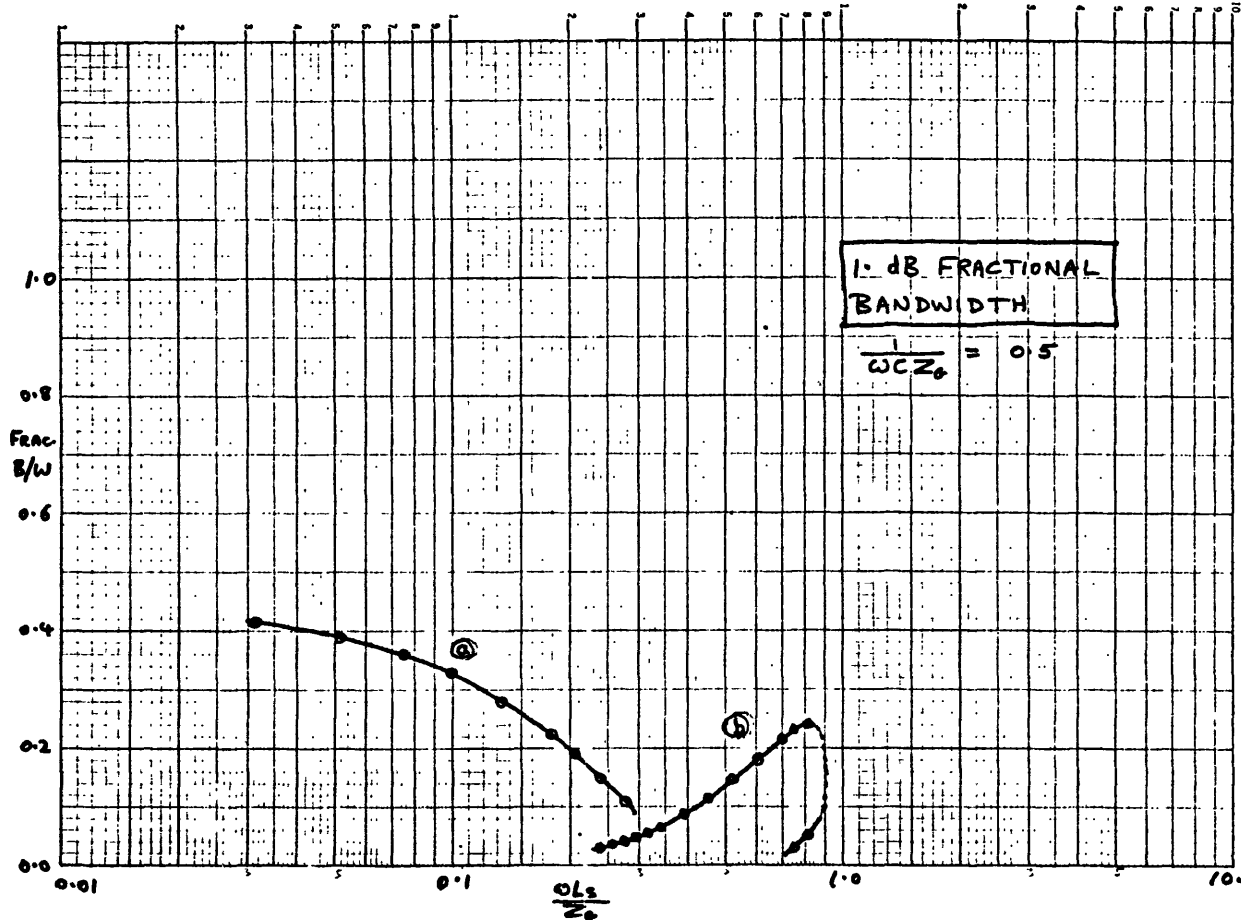
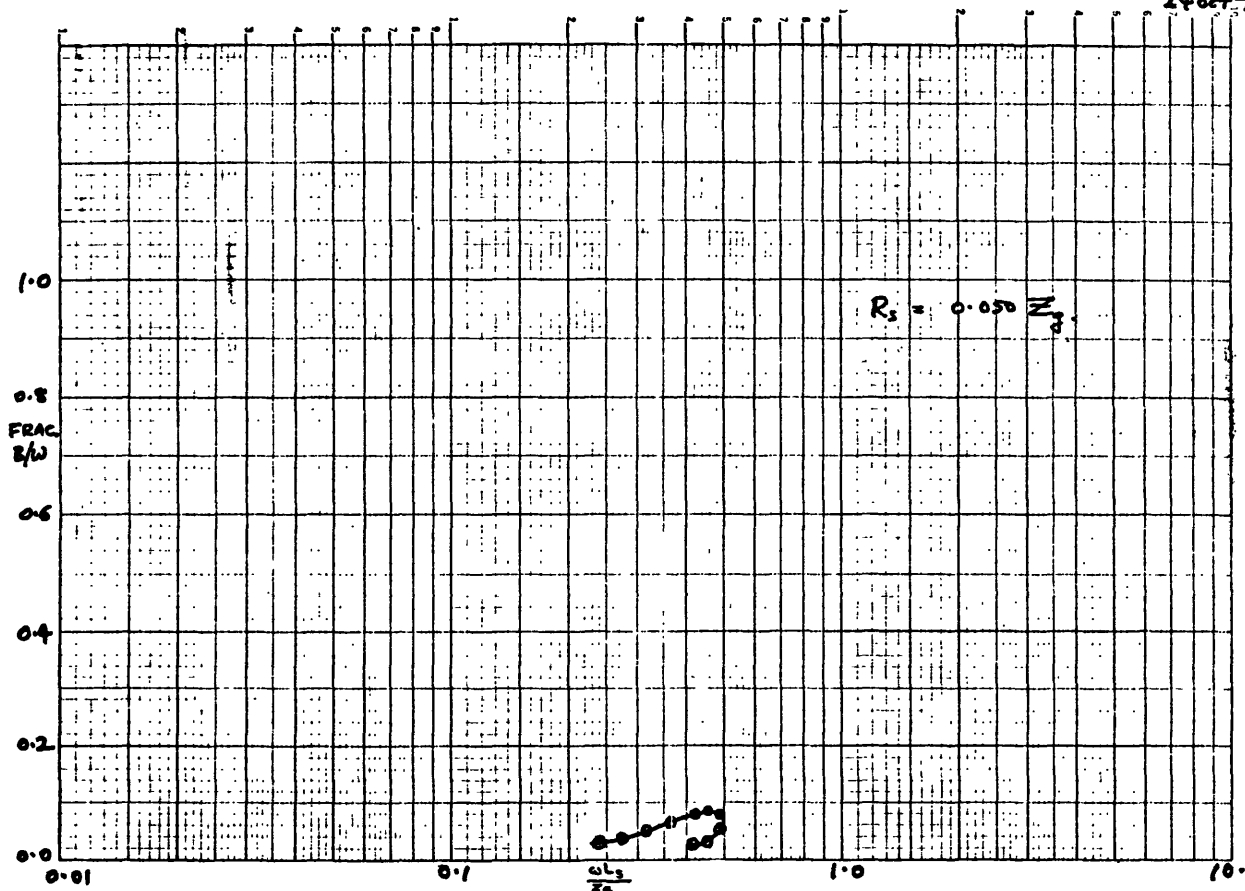


FIG. A2.5

$\frac{1}{\omega C Z_0} = 0.2$

ARK
MCM38W
24 OCT 71



APPENDIX 3: CONVERSION LOSS DEGRADATION CURVES

These graphs give the component of the conversion loss due to energy dissipated in the series resistance of the diode, for matching conditions as given in Appendix 1. For a broadband mixer this quantity (in decibels) adds to the fundamental 3 dB conversion loss, plus any loss due to mismatch, dissipation in the intrinsic junction resistance, and loss due to energy conversion to unwanted sideband frequencies.

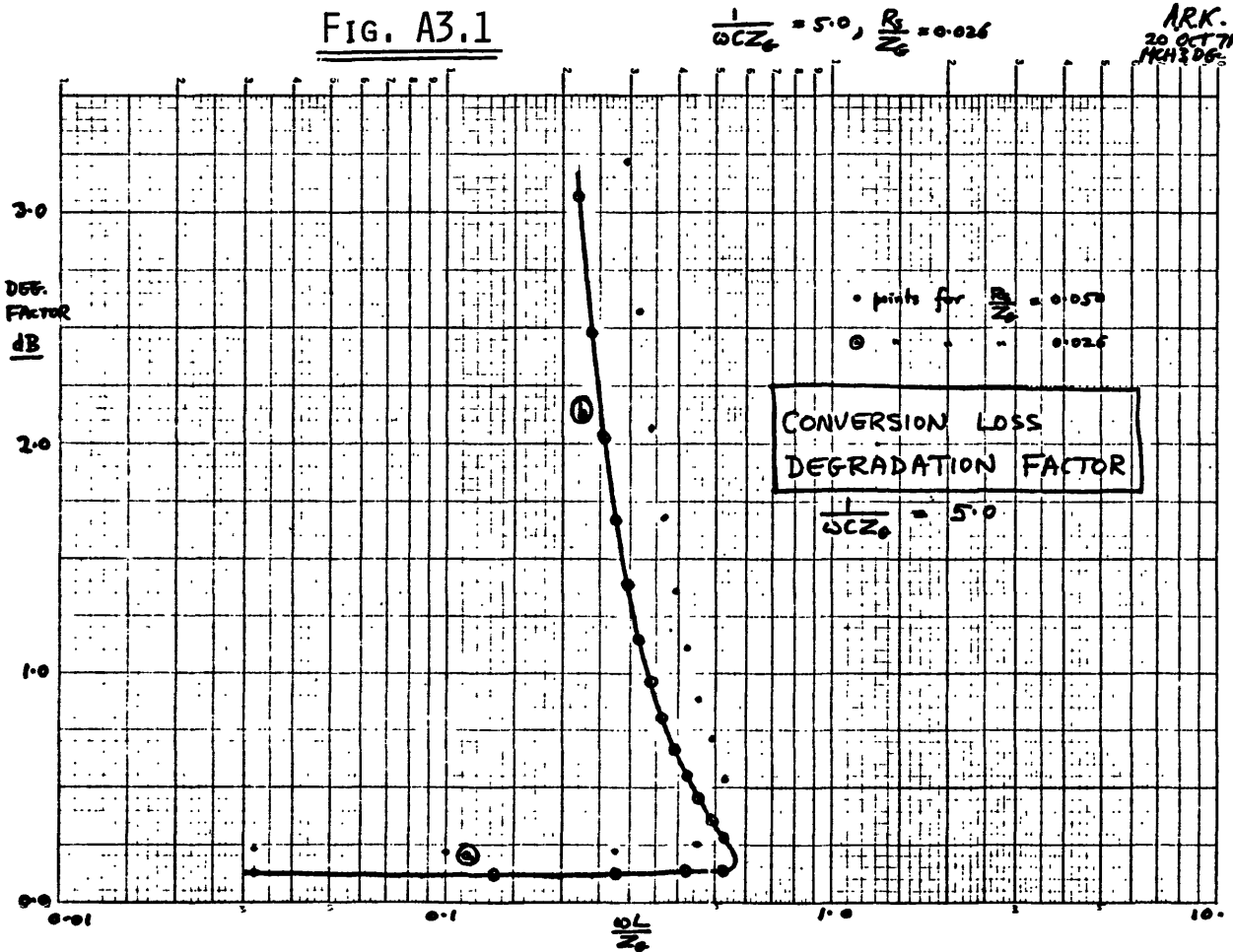


FIG. A3.2

$\frac{1}{\omega C Z_0} = 2.0$

ARK
20 Oct 71
MCH:SDP

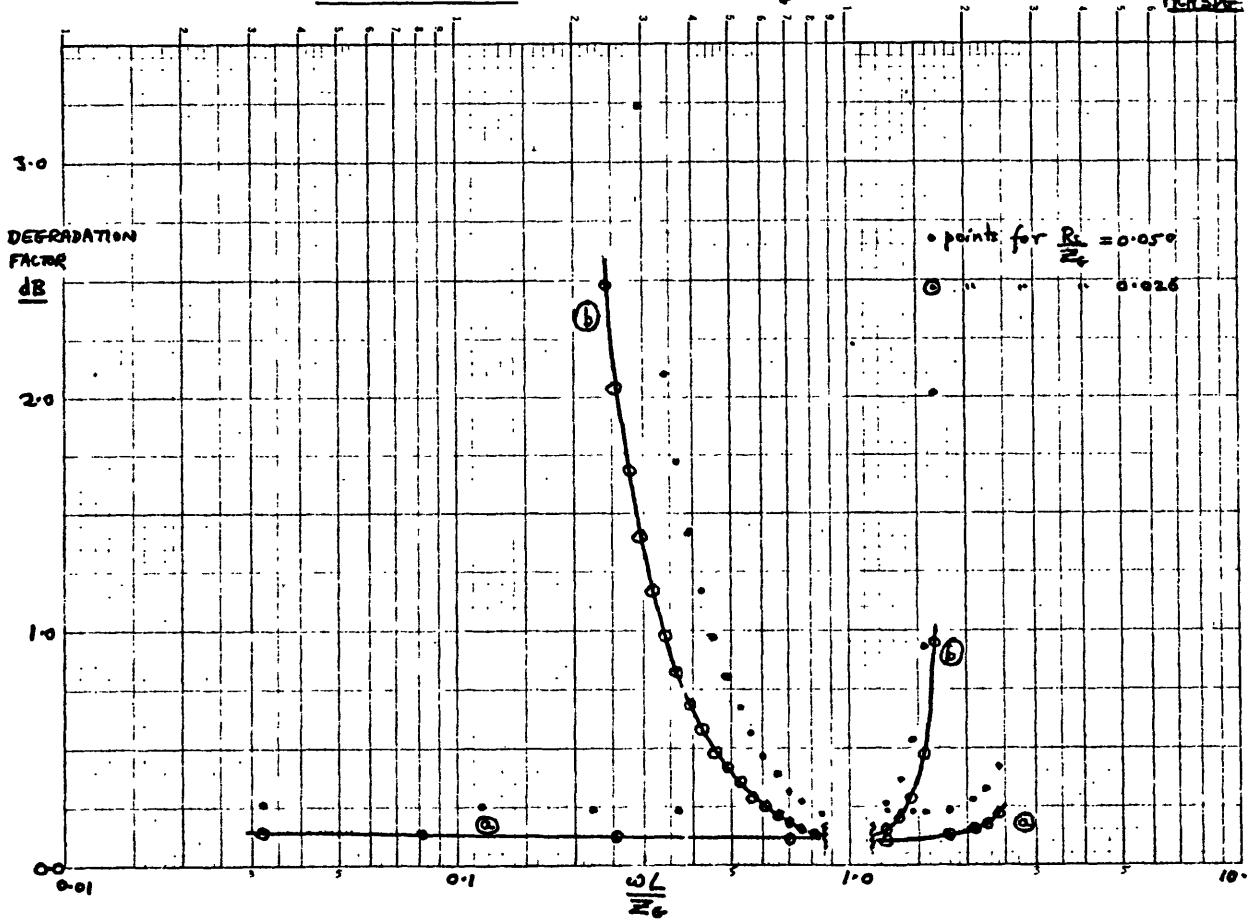


FIG. A3.3

$\frac{1}{\omega C Z_0} = 1.0, \frac{R}{N} = 0.025$

ARK
20 Oct 71
MCH:SDP

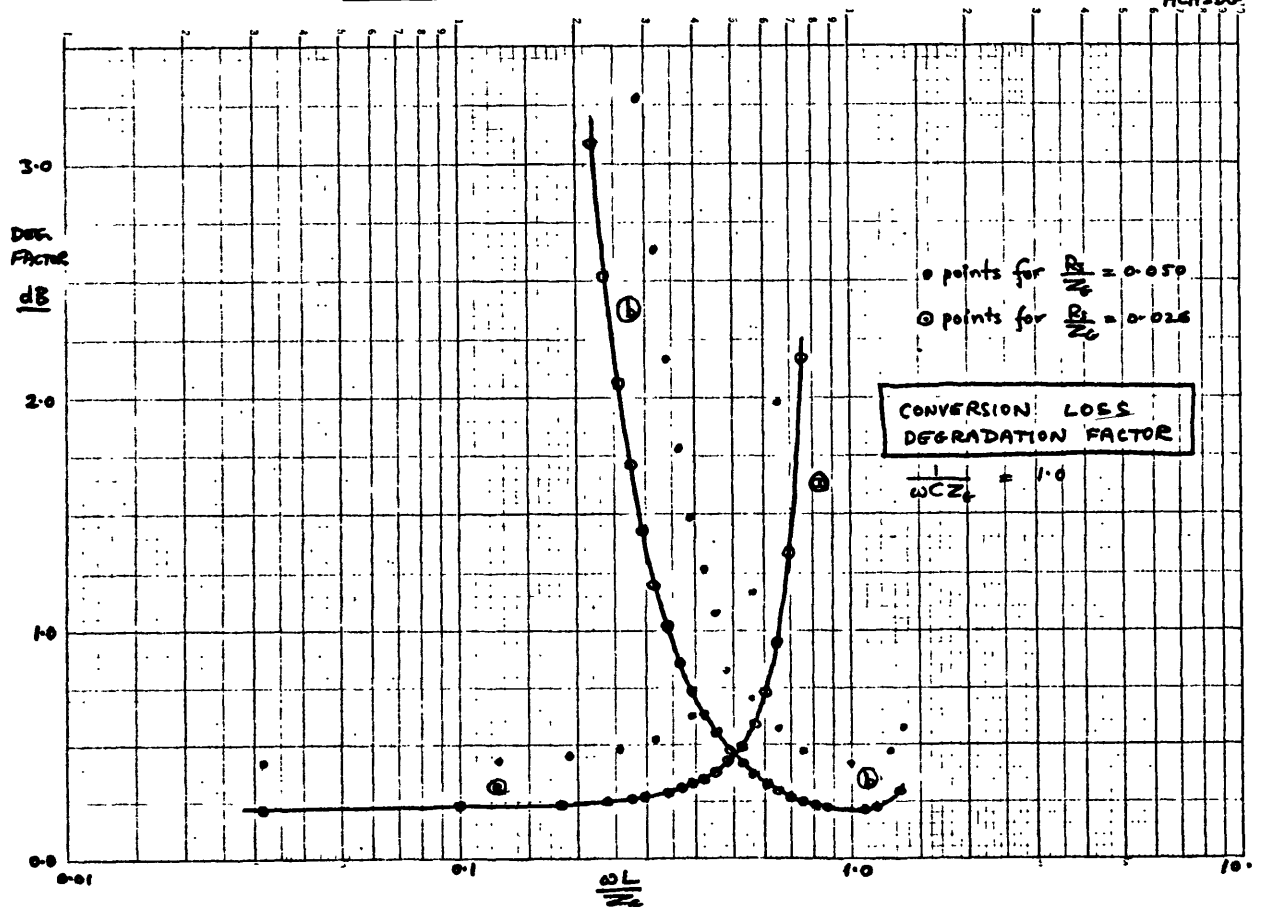


FIG. A3.4

$\frac{1}{\omega C Z_0} = 0.5, \quad \frac{R_0}{Z_0} = 0.026$

ARK
20 Oct 71
MCH3D6

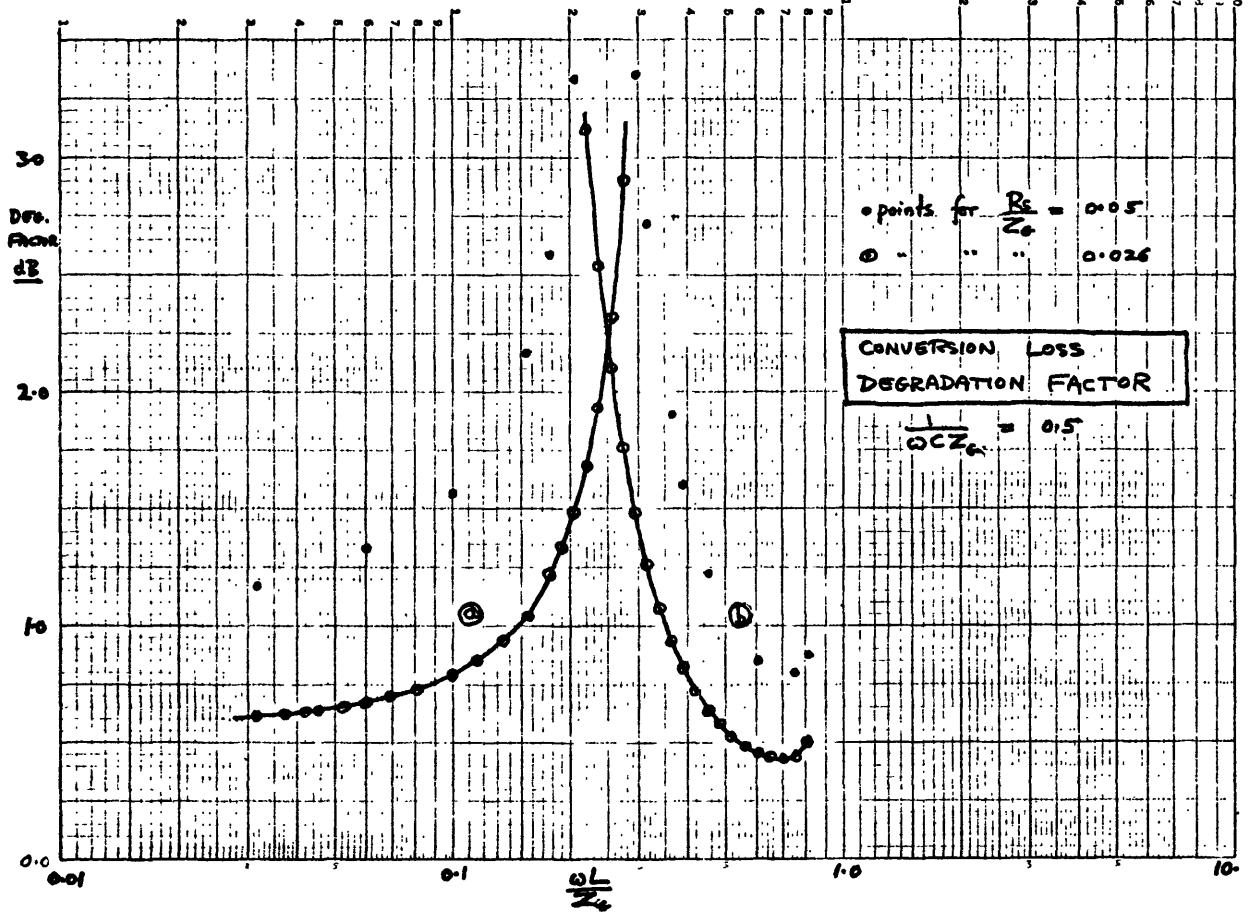
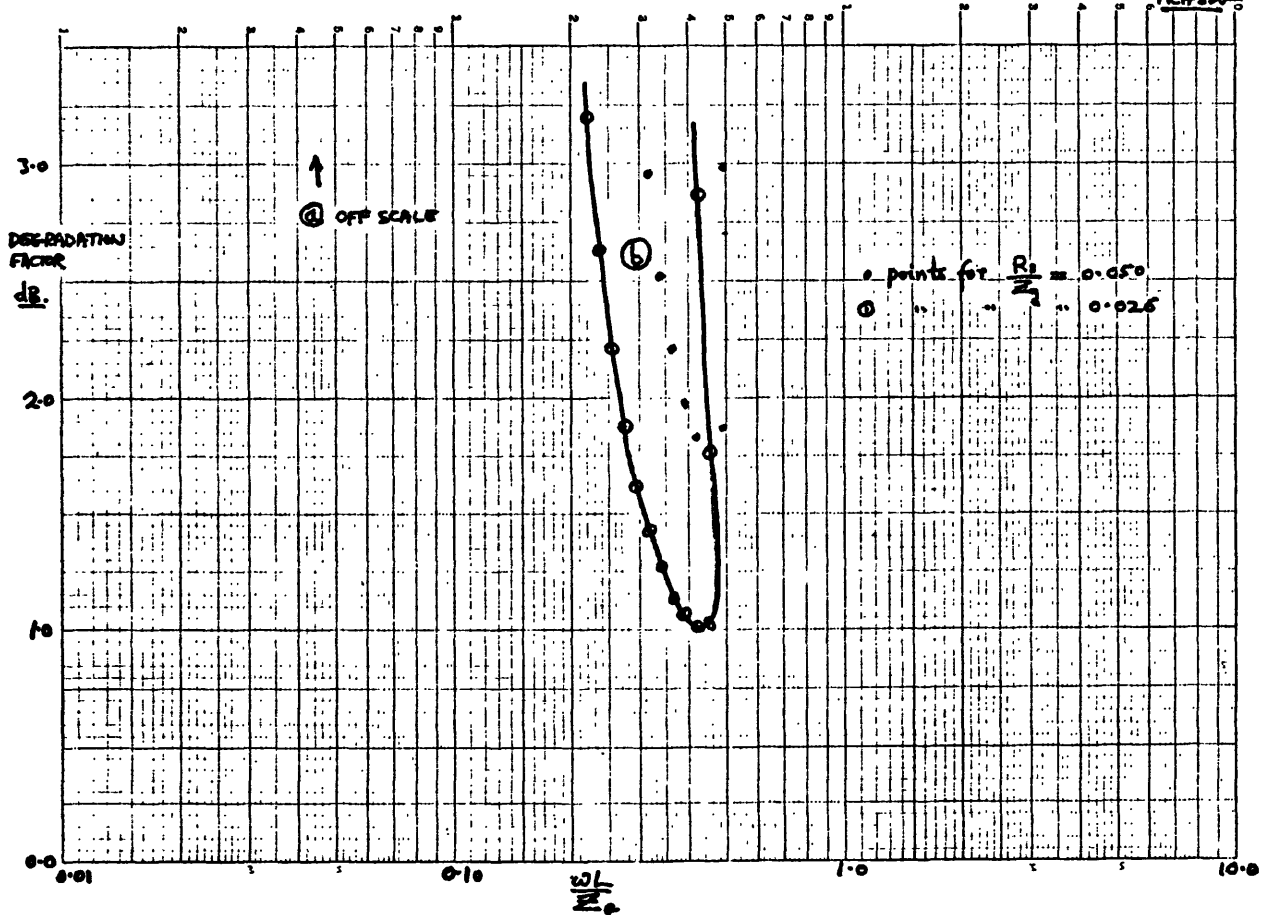


FIG. A3.5

$\frac{1}{\omega C Z_0} = 0.2$

ARK
20 Oct 71
MCH3D6



APPENDIX 4: PHOTOLITHOGRAPHY ON CHROME-GOLD QUARTZ

CLEAN

1. Rinse 1 min. in hot NaOH (tweezers also).
2. Rinse 1 min. in dist. H₂O (tweezers also).
3. Rinse again 1 min. in fresh dist. H₂O (tweezers also).
4. Place on clean microscope slide to dry. Dry tweezers.
5. Rinse 1 min. in boiling acetone.
6. Hold in tweezers over hotplate to dry (this prevents moisture from condensing as the evaporating acetone cools the substrate).

APPLY
RESIST
AND
PRE-
BAKE

7. Set oven to 80 °C (175 °F).
8. Place cleaned substrate on spinner.
9. Turn off all lights except yellow safe-light (pull venetian blinds to keep daylight out).
10. Drip resist liberally all over substrate.
11. Start spinner -- spin 1 1/2 min.
12. As spinner stops remove fine cobweb of resist (often suspended from spinner screws) using fine tweezers.
13. Place substrate on clean microscope slide.
14. Bake at 80 °C for 10 min.
15. Remove from oven. Do not expose unnecessarily to light.
16. If anything goes wrong, remove resist with Kodak Thin Film Rinse and repeat from Step 5.

EXPOSE
RESIST,
DEVELOP
AND
POST-
BAKE

17. Safelight only.
18. Place substrate on a clean microscope slide. Place negative(s) on the substrate, emulsion (dull) side against the gold. Hold negative down with another clean slide on top.
19. Expose 4 min. with 2 x 15w U/V tubes 2 to 3" from work.
20. Develop 1 min. in Kodak Ortho Resist Developer with agitation.
21. Rinse 1 min. in Kodak Thin Film Resist Rinse with agitation (especially important to agitate when first immersed).
22. Normal light now ok. Inspect image under microscope. If no good remove resist with Kodak Microneg Resist Thinner and go back to Step 5.
23. Bake resist 20 min. at 130 °C. Resist can now only be removed with stripper.

ETCH

24. Gold etch with agitation for ~ twice as long as it takes for pattern to appear etched.
25. Rinse in distilled water.
26. Chrome etch with agitation for ~ twice as long as it takes for gray chrome film to vanish.
27. Rinse in distilled water.
28. Rinse again in clean distilled water.
29. Inspect image under microscope.

RESIST
REMOVAL

30. Hot J-100 with agitation.
31. Rinse in acetone with agitation. Repeat from Step 30 if not clean.
32. Hot Shipley 1112 diluted 1:1 with water.
33. Rinse in distilled water.
34. Rinse again in clean distilled water.